Master Thesis in Geographical Information Science nr 160

Developing a Geographical Information System for a water and sewer network, for monitoring, identification and leak repair - Case study: Municipal Water Company of Naoussa, Greece

Konstantinos Sourlamtas

2023
Department of
Physical Geography and Ecosystem Science
Centre for Geographical Information Systems
Lund University
Sölvegatan 12
S-223 62 Lund
Sweden

Konstantinos Sourlamtas (2023).
Developing a Geographical Information System for a water and sewer network, for monitoring, identification and leak repair - Case study: Municipal Water Company of Naoussa, Greece.
Master degree thesis, 30 credits in Master in Geographical Information Science Department of Physical Geography and Ecosystem Science, Lund University

Level: Master of Science (MSc)

Course duration: *January 2022 until May 2023*

Disclaimer

This document describes work undertaken as part of a program of study at the University of Lund. All views and opinions expressed herein remain the sole responsibility of the author, and do not necessarily represent those of the institute.

Developing a Geographical Information System for a water and sewer network, for monitoring, identification and leak repair - Case study: Municipal Water Company of Naoussa, Greece.

Konstantinos Sourlamtas

Master thesis, 30 credits in Geographical Information Science

Supervisor:

David Tenenbaum

Department of Physical Geography and Ecosystem Science

Exam committee:

Ulrik Mårtensson

Department of Physical Geography and Ecosystem Science

Thomas Holst

Department of Physical Geography and Ecosystem Science

Abstract

This thesis presents the design and implementation of a Geographic Information System (GIS) for the Naoussa Municipality Water and Sewer Company for better water utility management.

The methodology contained field data collection like the valves, sewer manholes, hydrometers, hydrants with two ways, UAV photogrammetry and traditional surveying, the georeferencing process, photogrammetric processing, the digitization of old paper maps and the geodatabase design.

Moreover, the thesis investigates the resulting accuracy from the application of classical topographic methods in relation to that of UAV photogrammetry for mapping and collecting data on valves, hydrants, hydrometers, pipes and other water utility infrastructure.

The products produced from the use of such systems are characterized by high precision results. Accuracies ranging between the 0.15 - 0.29m have been achieved. The classical survey method gave more accurate results when compared with those produced by the UAV method. By using 85 GCPs, the accuracy of 4.5cm achieved in the final orthophoto.

Three indicative network management scenarios are implemented within the GIS environment. With these scenarios, the possibilities of managing the network are highlighted in terms of the coherence and integrity of the data, but also in terms of the introduction of new objects in the network and finally in terms of the network analysis possibilities that can be carried out by GIS.

This thesis tries to present and analyze the advantages and possibilities presented by GIS concerning urban water supply networks. It shows how a GIS can help the water company in its everyday work. Using GIS to manage the water company's utility data has allowed more flexibility over the previous analog system when analyzing data, and the management of the water network is more efficient.

Keywords: Water and sewer network, GIS, UAV, surveying, photogrammetry, orthophoto, geodatabase

Advisor: David Tenenbaum
Master degree project 30 credits in Geographical Information Sciences, 2023
Department of Physical Geography and Ecosystem Science, Lund University
Thesis nr 160

Table of contents

List of Figures

List of Tables

List of Abbreviations

EU	European Union
EEA	European Environmental Agency
GIS	Geographic Information Systems
TST	Total station
GPS	Global Positioning System
UAV	Unmanned Aerial Vehicle
GNSS	Global Navigation Satellite System
RTK	Real Time Kinematic
GCP	Ground Control Point
GCD	Ground Sampling Distance
PVC	Polyvinyl chloride
RGB	Red/Green/Blue
HEPOS	Hellenic Geodetic Reference System
DEM	Digital Elevation Model
ESRI	Environmental Systems Research Institute
CPU	Central Processing Unit
GPU	Graphics Processing Unit
SCADA	Supervisory control and data acquisition
GGRS87	Greek Geodetic Reference System 1987

1. Introduction

Greece has been identified as one of the EU countries that will face major problems due to a lack of water in the future (Toreti et al. 2022). This fact has forced water services to upgrade water and sewer networks so as to minimize losses of water. By integrating sensors and systematically monitoring the situation of water loss, water services can limit the losses. Because the municipality of Naoussa has enjoyed an abundance of water (newsbeast,2018) the authorities did not feel the need to act. It is noteworthy that the water agency of Naoussa, with conservative calculations, records more than 30% losses of input water. The situation is getting worse as a result of drought in recent years and, in particular, due to the frightening reduction in rainfall this past year, which recorded a decrease of 50% (Toreti et al. 2022).

Water is one of the most significant utility services for people, which contributes to quality of life (Petroulias et al., 2016). Small water utilities have the obligation to distribute the water in a city and to manage, maintain and analyze the associated infrastructure. However, small water agencies often do not have the capability to have a Geographic Information Systems (GIS) system due to lack of funds, and personnel (Vega, 2009).

Small water utility organizations have and operate their assets through paper maps, where the characteristics and locations of their objects of interest are visible (Maidment, & Morehouse, 2002). These maps played a major role in the past for 4 purposes: 1) Recording the location of the system infrastructure, 2) tracking the engineering information of each asset, 3) maintaining a connection with customers, and 4) providing the capability for analysis of the water and sewer network (Maidment, & Morehouse, 2002).

Every utility industry is a potential user of GIS, since all utilities have spatial information. GIS contributes not only to finding and knowing the location of each asset accurately, but also to analyzing their attributes (Wang and Yin, 2008).

In this regard, GIS can provide the capabilities a water agency needs, information about their assets, both spatial and non-spatial. Organizations like water agencies spend large amounts of money and time on the maintenance and repair of their infrastructure (Sokratis, 2019). They can incorporate GIS into their systems, in order to save time and money from their budgets and ultimately have a GIS system in order to manage all their utilities (Fellers, 2013; Lates *et al.*, 2018). The municipality of Naoussa does not have a system so far for this purpose, and the utility departments are in need of a GIS system.

The future use and operation of GIS within the water agency of Naoussa will reduce the working time required for the production of maps, will ensure valid and complete knowledge of the networks, will reduce the response time to the needs and requests of the customers, will reduce the operating costs of the company, and will give access to all the departments for better strategic planning (Luca et al., 2016).

GIS for water and sewer network needs datasets, such as orthophotos, for the precise depiction of their elements on the field. They provide high accuracy, which is important for the quality of analysis (Anurogo *et al.*, 2017; Sokratis, 2019). They can be produced by using the traditional surveying techniques with total stations and GPS, but this demands time. Unmanned Aerial Vehicles (UAV) or drones can be used for the collection of accurate aerial images. Studies have shown that surveying methods are more time demanding, with more people needed for the collection of data in contrast with the UAV methods, while the accuracy is comparable (Anurogo *et al.*, 2017; Sokratis, 2019; Huber, 2021).

1.1 Aim and research objectives

Despite the fact that Geographical Information Systems are important tools for the management of water and sewer network, no such systems are currently used in the small water companies and in Naoussa's Water Company. Therefore, the aim of this thesis project was to implement a GIS system for the Naoussa Municipality Water and Sewer Company for better water utilities and to investigate two mapping ways for accurate collection of the water and sewer data.

Objective 1: Collect the spatial information needed from the two mapping methods (ground survey & UAV photogrammetry).

Objective 2: Compare the two mapping methods, with a comparison way, by Eyoh et al. (2019) that used a comparison between the two mapping techniques (UAV and ground survey) compared to referenced data.

Objective 3: Analyse the performance of the developed GIS for the water and sewer network by applying real management scenarios from the Naoussa Water Company.

2. Background

2.1 GIS in small water company

Geographic Information Systems (GIS) are a means of managing, organizing and combining a large volume of information with their simultaneous display in space (in the form of a map). Also, GIS can be used for recording and analyzing the ongoing condition of utility networks (Vega, 2009). They are the modern solution for immediate, efficient, valid and reliable management of water supply- sewerage networks throughout the world (Wang and Yin, 2008). The various elements of a water supply network can be introduced into a GIS with their spatial nature (points, lines, polygons) but also with the descriptive information concerning them (eg. pressures of nodes) (Vega, 2009). Therefore, GIS has become a significant tool for water and sewer utilities, and not only for mapping purposes, but for essential management.

Small municipal water companies are distributing water in sparsely populated areas and, in this context, manage the whole water distribution and sewer system for infrastructure, maintenance and analysis. The trickiest and most demanding part of these activities is the management of the associated infrastructure and utilities, especially for a small water municipal company (Fellers, 2013).

Also they have a tendency to have an old (and not digitized) water and sewerage system, as they tend to lack funds for the application of modern approaches. They have greater sensitivity to failure of water utilities, and sometimes their failures may last hours without water supply. But the people living in such small communities do not accept the release of wastewater on their streets (Vega, 2009). Previous studies (Crawford, 2012; Fellers, 2013) on the design, implementation and manipulation of a GIS system by a water company have shown that, often a large budget and many people are needed for the final creation of a GIS system for a water municipal company.

Cannistra (1999) and Shamsi (2005) have pointed out many GIS applications from which a small water company would benefit. It would benefit from a new and updated water facilities map and creation of maps. By applying this, a small water company would replace the outdated and inefficient old paper maps that they currently use in their everyday work. As Yan et al., (2008) said, GIS allows water utilities to create new vector features with information, spatial and non-spatial, use topology and create helpful and useful printable maps that will help workers and managers in their everyday work:

1. Before work in the field (autopsy, repair, consumer request) a map will be printed from online GIS.
2. In the field, the actual situation will be compared with the GIS map.
3. Variations will be marked on the map.
4. On return to the office the corrections will be forwarded to the GIS department and entered.

Another important GIS application for a small water company that Cannistra (1999) and ESRI (2016) point out is the relation to the customer billing data, mail list and access of assets inventory. Information for customers should be accessible in the GIS application of a small water company (Cannistra, 1999). This can be done with several ways like by the locations of the building, by its address and by the location of hydrometers (Cannistra, 1999).

2.2 Geodatabase creation

For the important step of database implementation, and the most difficult part of GIS development, the database should be understandable and useful for everyone that use it (Shamsi, 2005). Shamsi (2005), points out three basic steps in the design of the database for a GIS. The first step contains the conceptual planning and the idea and design, the second is the logical design that is dependent on the software, and step three is the design itself that relate to the hardware and is the structure and content of the database (Shamsi, 2005).

2.3 UAV mapping techniques and data collection

The issue of identifying the most accurate way of mapping the water and sewer objectives was investigated. The evolution of technology in unmanned aerial vehicles (UAVs), as well as the development of new algorithms that are integrated into their data processing software, has resulted in its integration their use in the mapping of assets of a water company that are visible on the surface. The reasons that led to this are the simplicity of their use and their speed in relation to the now classical topographic methods (Anurogo et al.,2017).

The Naoussa water company is a rural company that has no resources and funds to create and implement a GIS system in the way that a larger water company would do so. So in order to properly succeed, the methods that have been used should be accurate, but also possible to employ at a low cost. Rayburn (2004) started to collect data on valves and hydrants from the city of Lufkin, Texas by using a sub-meter accuracy GPS tool and the pipelines and water mains were digitized by georeferencing old paper maps that created during the construction of the water and sewer system. The same methodology was used by Lyon, T. and Clifford (2008) for the Hardin County Water Company. Crawford (2012) used the same methods except he used aerial photography as a background for the digitization of valves and hydrants.

According to Sokratis, (2019) UAV-based photogrammetry techniques can provide the lowest cost, but a still sufficiently accurate method for the collection of data on the surface. The latest technological advancements have shown that the UAVs are equipped with a GNSS receiver along with high resolution cameras (Sokratis, 2019).

However, this kind of photogrammetric method requires the collection of Ground Control Points (GCPs) in order to georeference the images that have been acquired during the flight. These points are large, visible markers that are placed evenly distributed in the area that the flight is conducted (Sokratis, 2019). Then, using a GPS and the RTK method, the coordinates of these points are calculated and are used for the best accuracy of the final accurate basemap.

Using a UAV based photogrammetry technique for data collection, the outcome can reach the high accuracy of 2-5cm, according to (Anurogo *et al.*, 2017) and have significant advantages over other methods like the classical surveying method. In this way, the collection of data for the water and sewer network have been collected more quickly and with decent accuracy (Anurogo *et al.*, 2017; Sokratis, 2019).

3. Study area and data

3.1 Study area

This study was conducted in Greece and the study area covers the region of Naoussa. Naoussa or, officially, the Heroic city of Naoussa, is located in the region of Central Macedonia, and is built at the foot of Mount Vermio. It is a mountain town and according to the latest census, the largest mountainous urban center in Greece. According to the 2021 census, the population is 20960 inhabitants. Naoussa is located in the western part of Imathia, 22 km north of the capital of the prefecture of Veria (Figure 1). It is located 90 km northwest of Thessaloniki and 32 km south of Edessa. It is built at the eastern foot of Mount Vermio. The Arapitsa River is the most important aquifer in the area and crosses the city (Municipality of Naoussa, 2023). The geographic coordinates are 40°37′50″N 22°3′51″E.

The modern water supply network of Naoussa was initially constructed in 1981. The network is of a mixed type (closed and radial) which is due to its fragmentary construction without preliminary technical study. In the year 1991 a study was commissioned for the reconstruction of the existing water supply network. It was suggested that some interventions be made to modify pipelines in a part of the network. Until then the length of the pipelines of the aforementioned part of the network was 3.27 km. The study proposed to install new pipes and replace some old ones for the network to meet the future needs of the population. The total length of the complementary works amounted to 7.8 km of which 4.53 km were new pipelines and the remaining 3.27 km were replacements. The pipes that used were made of PVC (polyvinyl chloride) class 10 atm with the following elements, F110, F90, and F63 for pipe diameter. Today the network consists of approximately 3990 water and sewer pipelines and 907 nodes and serves almost the whole area of the city of Naoussa.

According to The Water and Sewer Company of Naoussa, they serve over 12000 customers. Their main goal is to provide clean and drinkable water to everyone. They do not utilize GIS and use old engineering drawings that are inaccurate and not easily understandable, since they were made by hand. The Water and Sewer Company of Naoussa wishes to utilize GIS in order to replace the outdated maps and to know exactly where the elements of its water and sewer network is located, but do not have the funds and the personnel to succeed it.

Figure 1: Approximate location of the study area in the region of Naoussa (source: maps.Geodata.gov.gr)

3.2 Data

For the purposes of this project, an extensive collection of data for the water and sewer network were collected and stored in a geodatabase. Data on valves, hydrants, hydrometers, pipes and others were collected in two ways: Firstly, they were collected with a geodetic GPS tool and secondly, by using photogrammetry and drones. Thus, the datasets that were used are UAV images, total station/GPS measurements, ground control points (GCPs), old paper maps depicting the water and sewer network, and cadastral vector data (Table 1).

Table 1: Datasets for the study

Datasets	Coordinate Reference System	Source
UAV Images (approx. 21.000)	Greek Grid/GGRS87, EPSG:2100	Collected with the drone flight
GCPs measurements (85)	Greek Grid/GGRS87, EPSG:2100	Collected in the field
water and sewer data (6285 water & 8116 sewer)	Greek Grid/GGRS87, EPSG:2100	Collected in the field
Paper maps (421)	paper format	Naoussa Municipal Water Company
Cadastral vector data	Greek Grid/GGRS87, EPSG:2100	National Cadastral Agency of Greece

3.2.1 UAV images

Several UAV images of the study area were collected during a number of 58 flights, covering the study area. Since the UAV that was used has a 30 minute battery limitation, several flights was done with more than one extra battery. The number of images needed depends on the size of the study area. The images were Red/Green/Blue (RGB) and in jpeg format from a FC330 camera mounted to a DJI Phantom 3 drone, which include a GNSS receiver and a has maximum flight time of 30 minutes. In each of the flights that took place, the flight altitude was 50 meters, and the flight speed 5.2 m / s. The overlap of the photos was set to 75%.

3.2.2 Traditional Surveying technique

According to the methodology followed, the GNSS receiver remains at one point and collects primary data from the available satellites of the GNSS system used (in our case the GPS). The GPS receiver is placed at points of interest for a few seconds (e.g. 20 seconds) at each. Then in the office, the required comparison is made, determining the difference between the field recordings and determining their coordinates in comparison to that of the fixed receiver in the Hellenic Geodetic Reference System of 1987. This uses data from its Hellenic Positioning System (HEPOS) KTIMATOLOGIO SA. In this way, the receiver in the field receives, at the same time, data from satellites and the location of known coordinates of points of interest for the water company. In the present thesis, GNSS satellite tracking receivers were used, which are now the main means of determining precision coordinates in topographic applications (1-3 cm).

3.2.3 Ground control points

Next, the ground control points had to be defined. As such points were selected that would definitely be recognizable in the UAV photos, their coordinates could be measured with great accuracy. The distribution of points was uniform across the length and width of the study area. To determine the coordinates of ground points, they were measured by using a GPS RTK-GNSS tool for accurate measurement of the location of each GCP x-y-z location. In this way the images were placed more accurately in the study area. For each UAV flight, 6 GCPs were evenly distributed (Figure 2).

Figure 2: Distribution of GCPs in a part of the study area for a UAV image set.

3.2.4 Paper maps

The municipal water company of Naoussa has previously used only paper maps for the identification and location of the pipes and their characteristics underground (Figure 3). These old, but valuable, paper maps are the only evidence of what is and where is it for the water and sewer network. Therefore, in order to collect the data for every pipeline and valve, these maps need to be digitized correctly. During the digitization in ArcMap, snapping lines (water and sewer pipes) to points (valves, manholes) were digitized since the point features were collected in the field and by photogrammetric processing.

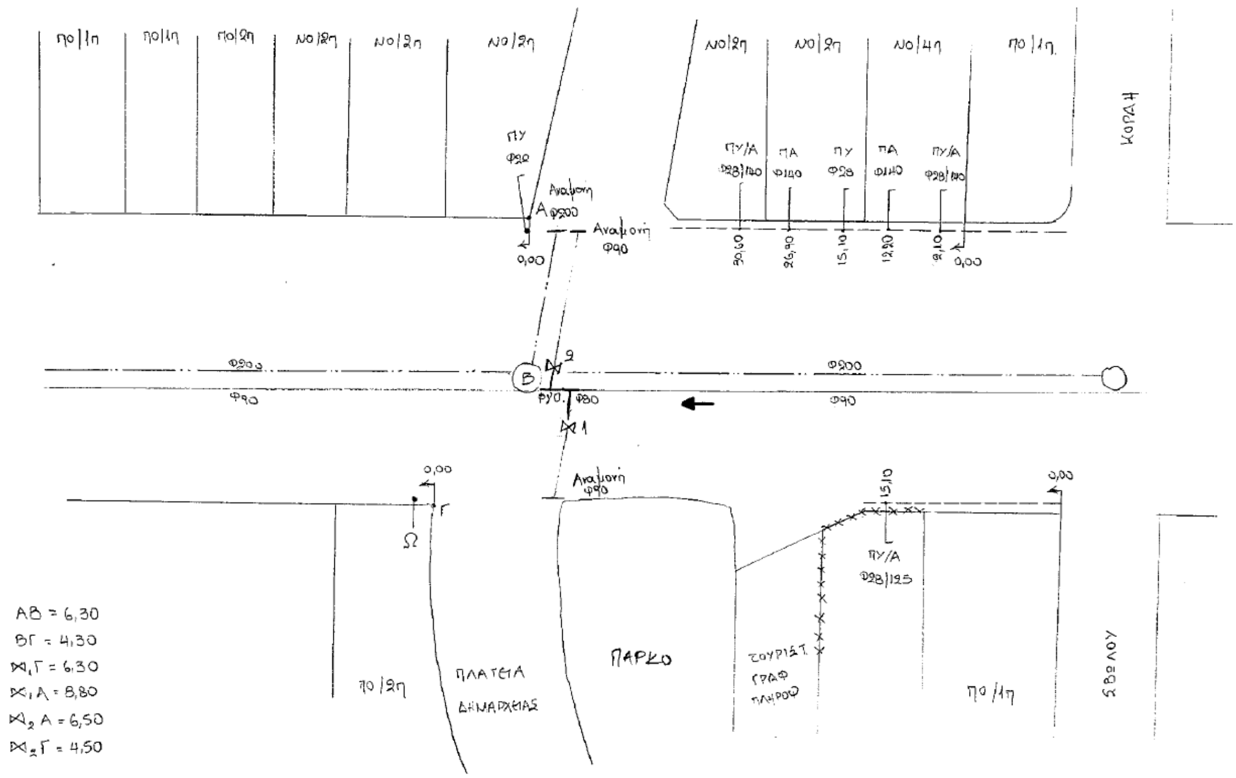

Figure 3: An example paper map with information about water and sewer network (source: Municipal Company of Naoussa).

3.2.5 Cadastral data

For the connection of each property and customer with the water and sewer network that was constructed, the cadastral data for each property and, building was acquired from the National Cadastral Agency. According to the National Cadastral Agency, they were produced by field surveys with 2.5 cm accuracy. In this way, the water company have been able to identify where its customer lives, what are the characteristics of the pipeline for each customer's building.

4. Methodology

4.1. Geodatabase design

This phase of the project, the geodatabase design, began by checking all the available data, gathered in the field and by the digitization of the old paper maps. The feature classes were determined by which water and sewer network data are important and significant for the Water Company. Also, each feature class has specific attributes that correspond to the needed information for each feature class and these include any information that the Company would like to keep track of in the future. Specifically, the feature classes planned at the thesis time were pipelines, valves, tanks, hydrants, water meters, and sewer manholes.

Moreover, other data like buildings, cadastral data, roads etc, were obtained from the National Cadastral Agency. The basemap was the orthophoto that was created from the photogrammetric processing and the DEM. All the datasets are in the Greek coordinate system Greek Grid, GGRS87. The following tables illustrate the attributes for the water network, sewer network, valve, sewer manhole, fire hydrant storm water manhole and House water meters.

Table 2 shows the attributes that were collected for the water and sewer network feature class. The Water and Sewer Company wanted to collect the pipe material, diameter, address and length from paper maps.

Table 3 shows the valve feature class. The information collected from the field and from orthophoto and from the company personnel. It can be used to shut off the water mains.

Table 4 shows the attribute information for the water meter feature class. The locations were collected with GPS and the customer information was collected from the company's database.

Table 5 shows the fire hydrant feature class and its engineering information. GPS system was used to collect them and can be used in a fire incident.

Table 6 depicts the sewer manhole feature class engineering information and they were collected in the field using the GPS system and with the orthophoto from the photogrammetric processing.

Table 7 shows the consumers sewer manhole feature class and its attribute information which is located outside of each house and connect with the main sewer network pipe. They were collected in the field using GPS and from the 2cm accuracy orthophoto.

Table 2: Water and Sewer network feature class information.

Feature Class:	Water network and Sewer network
Description:	Network of water mains in GIS system.
Data Source:	Digitized data
Geometry Type:	Polyline
FID	HISTORY OF ERRORS
SHAPE	ADDRESS
DIAMETER	DATE OF SETUP
DEPTH	OBSERVATIONS
MATERIAL	STATUS
LENGTH	X,Y

Table 3: Valve feature class information.

Feature Class:	Valve feature class
Description:	Shut of valves on the water main
Data Source:	collected on the field and from orthophoto
Geometry Type:	Point
Description	address
observations	X,Y.Z
History of errors	Diameter
Condition	Setup Date
Type	

Table 4: Water meter feature class information.

Feature Class:	Water meter feature class
Description:	Water meters in the GIS system
Data Source:	Located with GPS system
Geometry Type:	Point
Address	X,Y,Z
Name of recipient	Code
Hydromrter code	Type
Information	History
Setup date	Last measurement Date
Last measurement(m3)	

Table 5: Fire Hydrant feature class engineering information.

Feature Class:	Fire Hydrant Feature class
Description:	Fire Hydrants
Data Source:	Located with GPS system
Geometry Type:	Point
Address	X,Y,Z
Location	Type
Connection type	History
Mode	

Table 6: Sewer Manhole Feature Class Information.

Feature Class:	Sewer Manhole
Description:	Sewer Manholes located in sewer pipe
Data Source:	Located with GPS system and UAV
Geometry Type:	Point
Description	X,Y,Z
Address	Information
History of errors	Diameter

Table 7: Consumer Sewer Manhole Feature Class Information.

Feature Class:	Consumer sewer manhole
Description:	Consumers Sewer Manholes located in household sewer pipes
Data Source:	Located with GPS system and UAV
Geometry Type:	Point
Description	X,Y,Z
Address	Information
History of errors	Diameter
Length	

4.2 Field data collection

For the collection of data, like the valves, sewer manholes, hydrometers and hydrants from the city of Naoussa, a meeting was held with Water and Sewer Company personnel in order to determine each route through the city, and for a better determination of which water meter belong to what address and what customer code. Also, existing old maps of the water and sewer network were printed for better location of each objective.

A sub-meter GPS and the RTK method was used in order to acquire the location of each element on the surface for the water and sewer network. The use of RTK (Real Time Kinematics) techniques during the last decade has become widespread. It is based on the determination of 3-D position of points using GPS in real time, with an accuracy that for the horizontal position usually ranges from 1-2 cm. The RTK technique is based on the existence of reference stations and moving GPS receivers (known as the rover) which communicate with each other using radio signals.

4.3 UAV Measurement procedure

The first stage of the measurements involved the creation of the flight plan. Given the size of the study area and the capabilities of the available UAV, it was decided to carry out 5 flights per flight (one 90^0 and four 45^0 for every direction).

In each of flights that took place, the flight altitude was set to 50 meters, the flight speed to 5.2 m / s, the overlap of the photos during the two routes have been about 75%, and the angle of the camera have been oriented at 90 degrees vertical in one flight and 45 degrees in the other 4 flights.

Next, the 85 ground control points were defined across the study area. Points were selected such that they would definitely be recognizable in the UAV photos and their coordinates was measured with great accuracy. The distribution of points was uniform both in length and width in the study area (Figure 4). To determine the coordinates of ground control points a GNSS GPS was used (Figure 5).

Figure 4: The distribution of GCPs in the study area.

4.4 Georeferencing process

The implementation of the georeferencing process requires the determination of absolute coordinates using appropriate equipment. For the purposes of this work, the use of satellite navigation receivers (Global Navigation Satellite Systems-GNSS) was chosen. Also, the UAV DJI Phantom 3 is a complete platform that supports a fully automated flight scheduling, data collection and storage process and was used in the collection of the aerial images.

A GNSS system consists of satellites orbiting the Earth that transmit signals containing position and time data. Today there are various GNSS systems such as US-controlled GPS, the European Union-developed Galileo program, Russia's Glonass system and China's BeiDou.

The processing of the measurements requires the use of appropriate software, both for the extraction of the geographical coordinates of the points of interest and, mainly, for the application of the technique of photogrammetry and the creation of the digital elevation model of the study area.

In this thesis, ArcGIS was used, which is a product of the American company ESRI (Environmental Systems Research Institute). The basic application of ArcGIS is ArcMap which has the ability to create and edit maps, display and analyze geographical data, still has the ability to search and select spatial data, graphs, and maps for printing.

Figure 5: Example of a GCP measurement with GPS.

4.5 Coordinate system synthesis

First of all, it should be mentioned that all files imported into GIS in this project must have the GGRS87, the Greek coordinate system (Greek Grid) so that they can be used together automatically, thus facilitating the processing and analysis of the data. In this way, geometric operations can easily be performed without any considerations of coordinate system mismatches (calculation of distances, areas, valves, hydrants etc). The results can also then be integrated into any known geodetic coordinate system.

The ground checkpoints identified in the photos got the coordinates resulting from the processing of GNSS metrics. The checkpoints were placed in the correct place in each photo at which this point is visible. GCPs are generally used to identify commonalities in different photos as well as to reduce the whole model to an audience coordinate system. Then the orthomosaic was constructed.

4.6 Photogrammetric processing

The photogrammetric processing aims to generate a 3D surface of the area. For the photogrammetric processing of the selected photos, Agisoft PhotoScan software was used. The ultimate goal is the creation of the three-dimensional surface model of the study area and the orthophoto in order to digitize the water and sewer network elements. The process of photo editing and 3D making model includes the following stages:

1. The first step is to align the photos. At this point the software looks for commonalities in the photos while at the same time finds the position of the camera in the space for each photo, and improves the calibration parameters of the camera. The result is a sparse cloud of dots (figure 6). The GCPs that were collected in the field imported after the alignment step.

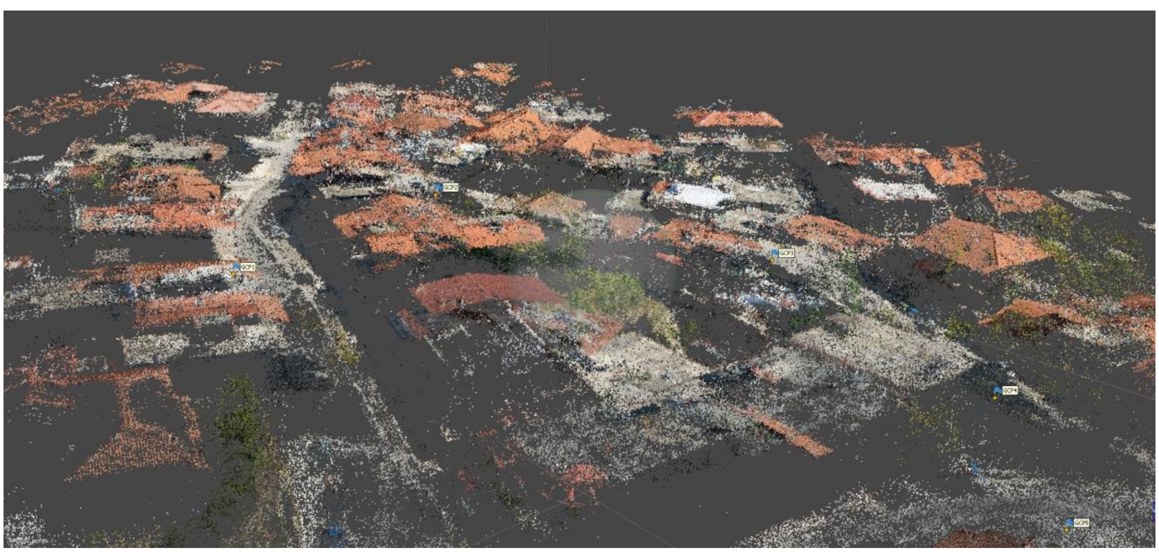

Figure 6: Alignment step.

2. The next step is to construct a dense point cloud. All available information is extracted from the aerial images in order to densify the sparse point cloud and use it to construct surfaces. Then the dense point cloud is produced (figure 7).

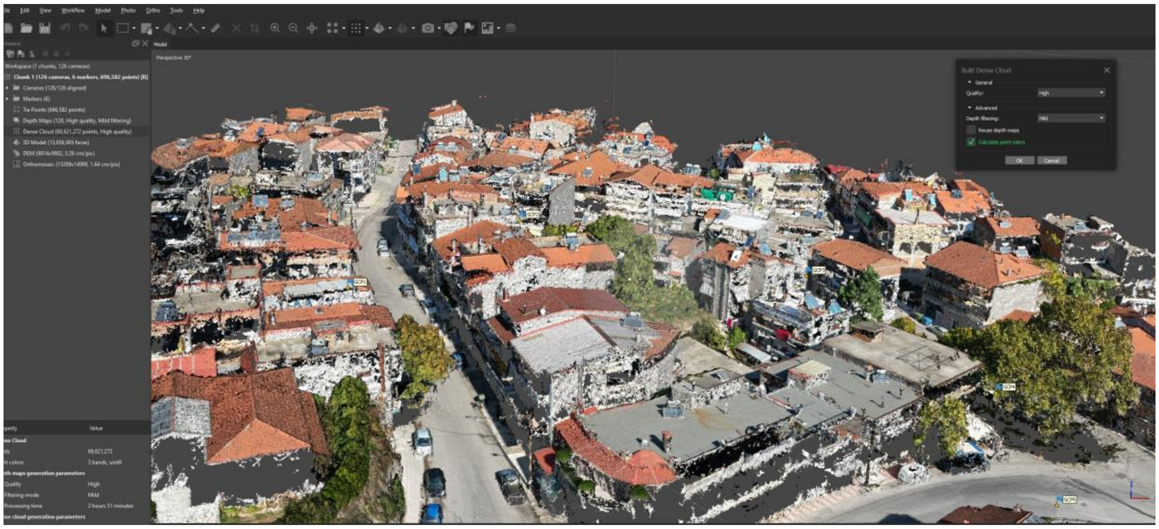

Figure 7: Dense point cloud processing step.

3. The third step is the construction of small surfaces (triangles) between the dense point clouds. The product is essentially a model of the real 3D object. The software constructs a three-dimensional polygonal grid, representing the surface based on the dense point cloud (figure 8).

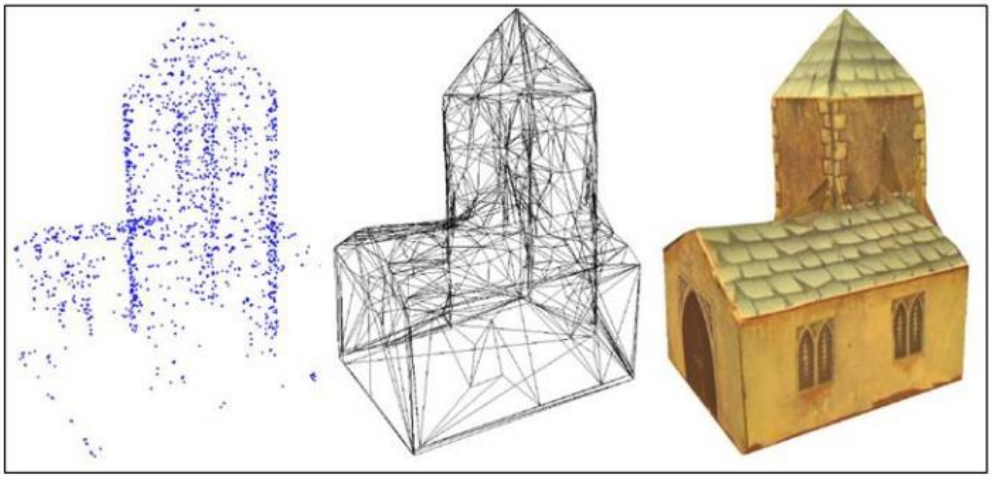

Figure 8: Creation of 3D Grid (Point cloud->Mesh->3D).

4. The creation of the texture of the relief essentially applies the existing photos to the 3D model that has been built (figure 9). The mosaic algorithm have been used to create the orthomosaic texture, according to which the details are not "mixed" by overlapping photos, but rather the most appropriate photo is used for any given location. For example, consider a case where the final pixel has the shortest distance from its center in an image as the ideal choice (Anurogo *et al.*, 2017).

Figure 9: Texture model.

5. Finally the orthophoto of the study area is constructed at the best possible cm accuracy (figure 10).

Figure 10: Construction of the Orthophoto.

4.7 Digitization of data

Data that cannot be collected in the field can be digitized using GIS software and paper maps that depict them (figure 11). The digitization of the water and sewer network was done using the ESRI's ArcMap 10.5.1.

All the data were in the Greek Coordinate System GGRS87, and as a background map the orthophoto from the photogrammetric processing were added. In that way, the water and sewer network were digitized from old paper maps and their attributes were added to the attribute table of each feature (figure 12).

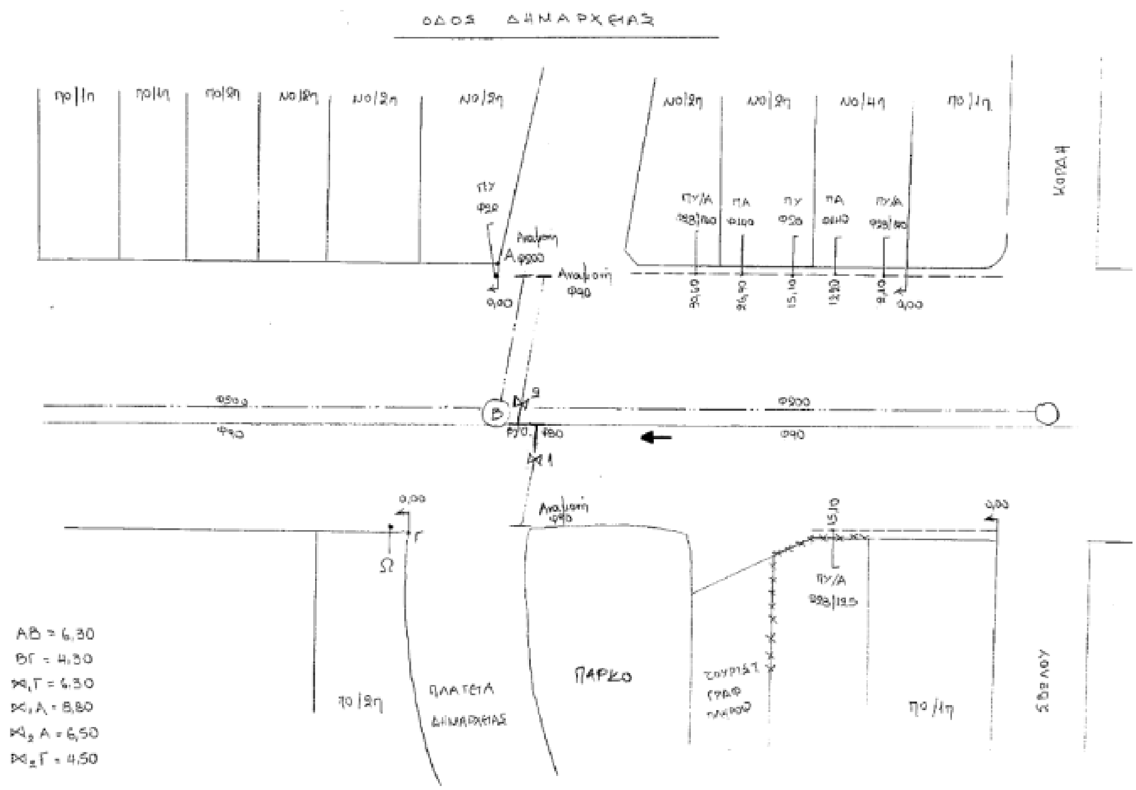

Figure 11: Example of an old paper map depicting the water and sewer network, manholes, valves and their attributes in a specific address.

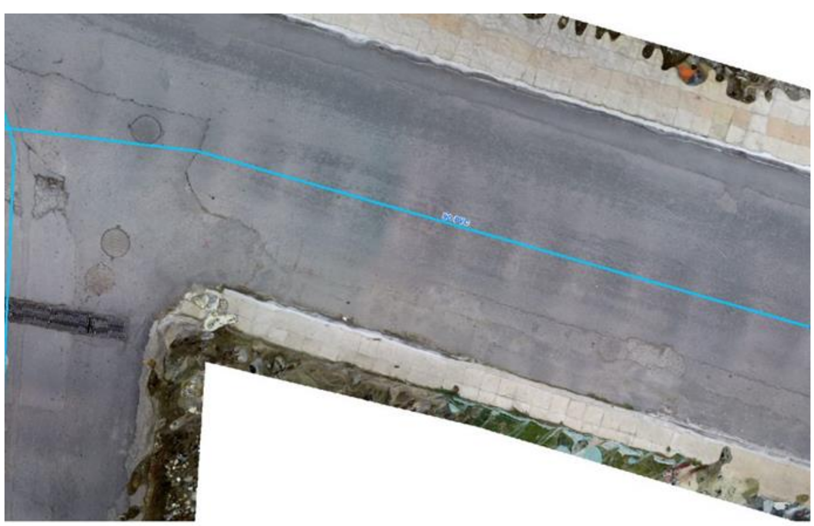

Figure 12: Orthophoto depicting the water and sewer elements and how the digitization process has been done.

5. Results

5.1 UAV Photogrammetric Data

58 flights were operated, each covering 9000 – 11000 m2 of the study area. Figure 14 shows the orthophoto that is produced as a result. With visual observation, there are clearly distinguishable constructions (eg buildings, roads) and parts of the water and sewer network that are on the ground (valves, sewer manholes, fire hydrants, storm water manholes and wells) (Figure 17).

The orthophoto map was produced only with the nadir shots (90 degrees). For its georeferencing, the 85 GCPs marked across the region (GCP 1-85) were used. The table 8 shows the final errors of the GCPs from the production of the orthophoto map as calculated by Agisoft.

Table 8: Ground Control Points Error, calculated by the Agisoft.

X error (m)	Y error (m)	Z error (m)	Error (m)	Error (pix)
1,05157	1,57169	3,34159	1,89104	3,83956

The accuracies in this particular process are good enough. This happens both due to the good determination of the coordinates and the better determination of the GCP center in the Agisoft. The total error of the GCPs is ±1.89 m. The RMS reprojection error was set at 3.84 pixels.

Next, the production of the DEM is done by taking as primary data those of the dense cloud of points. The final derivative (figure 13), which is also georeferenced, consists of an image with color differentiation where the elevation of the relief is also differentiated with a relevant legend.

After producing the DEM can also be used to create the orthophoto map (figure 14) with primary data from the digital terrain model. The GSD of the DEM is 4.04 cm/pixel while the orthophoto map is 4.5 cm/pixel. Its total production time was 12 hours.

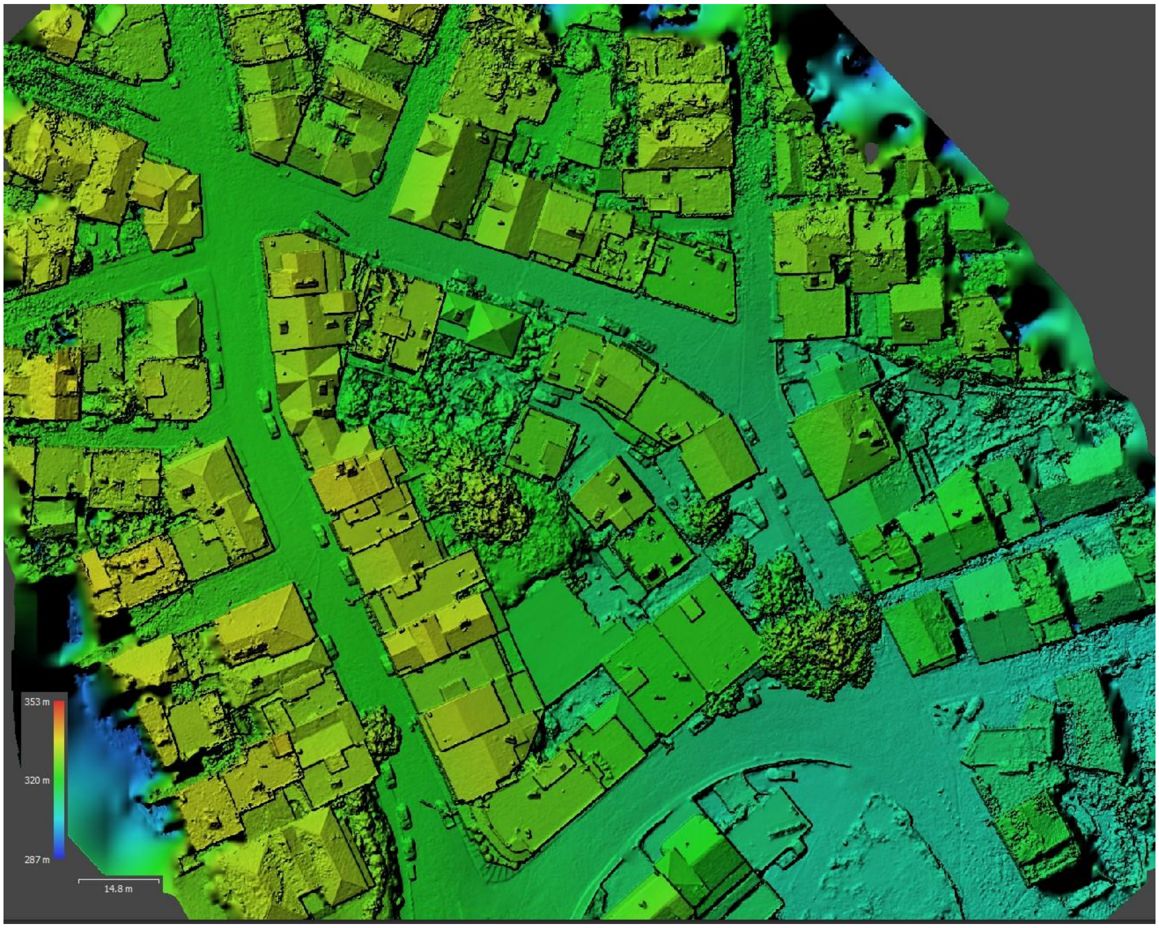

Figure 13: Part of the Digital Elevation Model (DEM).

Figure 14: Part of the orthophoto resulted from the photogrammetric process from the UAV data using GCPs.

5.2 Evaluation of the Mapping methods

85 GCPs were distributed along the study area and except from the orthophoto creation, were used as reference points for the comparison and accuracy check of the most accurate mapping method. They were measured with the statik GPS method (figure 5) where the GPS station is measuring every GCP for 15-20min for more accurate results. Table 9 is a part of the table in Appendix B that gives the reference coordinates for the comparison and accuracy check for both mapping methods.

Table 9: Reference coordinates for Accuracy check.

Label	Reference Coordinates		
	X(m)	Y(m)	Z(m)
GCP 1	336249.25	4499627.25	327.60
GCP 2	336253.97	4499626.96	328.39
GCP 3	336370.47	4499661.33	327.79
GCP 4	336373.88	4499658.89	327.81
GCP 5	336338.64	4499633.98	330.22
...			
GCP 84	336650.67	4499467.10	330.00
GCP 85	336628.72	4499510.49	329.32

For consistency purposes between the two mapping methods, the same number of GCPs was measured for each method, through ground survey with a total station and through photogrammetric software (Agisoft) in order to compare their accuracies in comparison to the referenced calculations.

During the ground survey method, for better accuracy, more than one measurement was done and the results averaged. For the photogrammetric method, after the image processing in Agisoft, the position of each GCP was zoomed and the coordinate in the center was measured. The coordinates of these GCPs from the two mapping methods are showed in the table 10 which is part of Appendix C table.

Table 10: Resulted coordinates of the ground survey and photogrammetric method of GCPs

Label	Total Station			UAV Photogrammetry		
	X(m)	Y(m)	Z(m)	X(m)	Y(m)	Z(m)
GCP 1	336249.17	4499627.35	327.10	336249.25	4499627.25	327.60
GCP 2	336253.99	4499627.19	328.58	336254.23	4499627.20	328.78
GCP 3	336370.49	4499661.47	327.92	336370.50	4499661.65	328.03
GCP 4	336373.94	4499659.02	328.01	336374.14	4499659.23	328.16
GCP 5	336338.78	4499634.09	330.28	336338.87	4499634.26	330.35
...						
GCP 84	336650.73	4499467.18	330.12	336650.77	4499467.40	330.19
GCP 85	336628.79	4499510.57	329.57	336629.00	4499510.81	329.70

While table 11 depicts the differences between the referenced coordinates and the two mapping methods which is part of the Appendix D table.

Table 11: Differences in coordinate values from the referenced coordinates.

Label	Reference-TST			Reference-UAV		
	δχ(m)	δy(m)	δH(m)	δχ (m)	δy (m)	δH (m)
GCP 1	0.08	0.10	0.50	0.08	0.11	0.13
GCP 2	0.02	0.23	0.19	0.26	0.24	0.39
GCP 3	0.02	0.14	0.13	0.03	0.32	0.24
GCP 4	0.06	0.13	0.20	0.26	0.34	0.35
GCP 5	0.14	0.11	0.06	0.23	0.28	0.13
...						
GCP 84	0.06	0.08	0.12	0.10	0.30	0.19
GCP 85	0.07	0.08	0.25	0.28	0.32	0.38
RMSE	0,152144031	0,161419	0,167997	0,266149	0,298766	0,293201

The mean difference of all GCPs for the ground survey (TST) method range in the X-coordinate is 15.21 cm, in the Y-coordinate is 16.15 cm, and in the Z-coordinate is 16.8 cm. For the UAV method, these values are 26.6, 29.87 and 29.32 cm respectively. At the edges of the models, as expected the errors grow large, while in some spots are even created due to the lack of overlap photos.

5.3 Digitization and mapping

The assets of the water and sewer utility network consist of valves, sewer manholes, hydrometers, hydrants, pipelines, storm water manholes and wells. Aerial data from drone, on site field collection with total station and digitization of old paper maps was used in mapping them as can been seen in Figure 15. Also the attributes of each asset were categorized in columns in each attribute table and includes many engineering information.

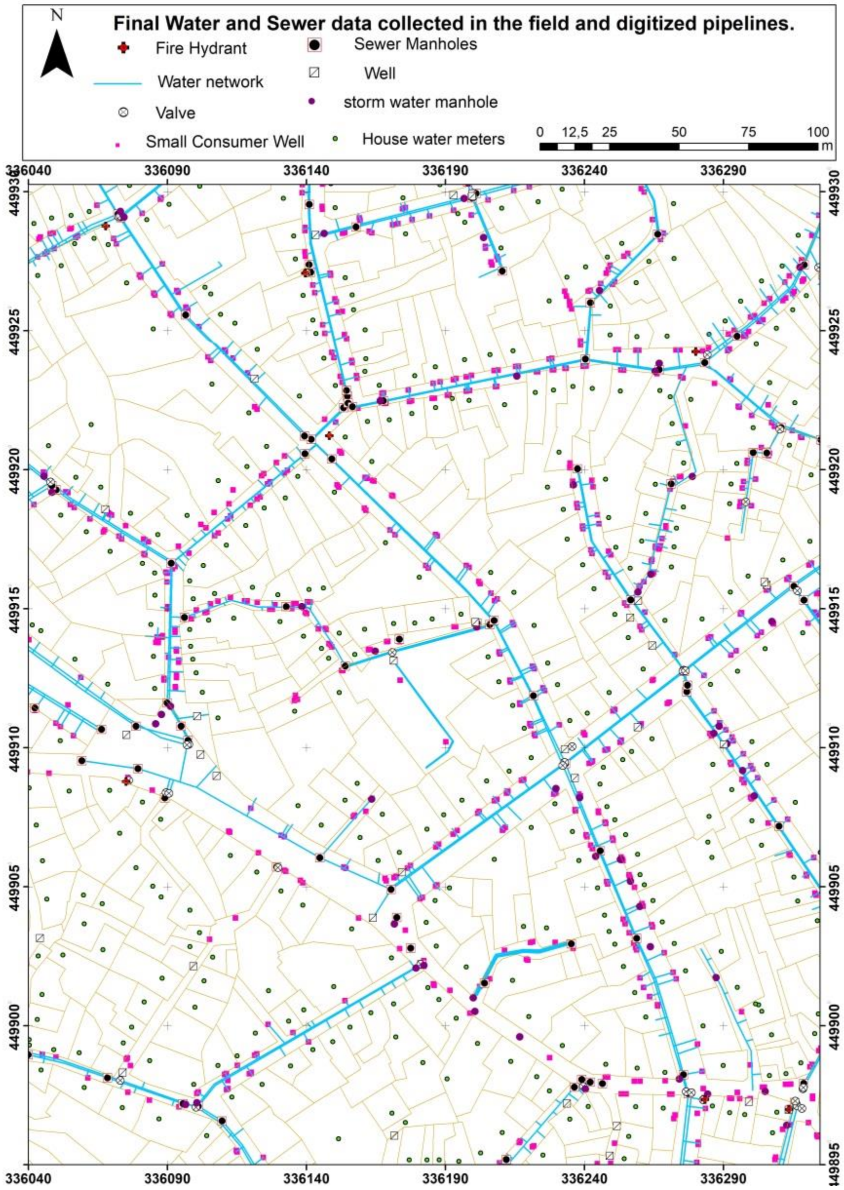

Figure 15: Collected data in a location of the study area (source: Water Company of Naoussa)

Assets like the water and sewer pipelines that cannot be mapped from aerial methods since they are below ground, were digitized based on the old paper maps that depict them. While digitizing them, the main idea was that they are aligned along the roads and were connected with the manholes and valves that were collected through the TST and UAV process. All pipes are connected properly from high to low diameter. The majority of them are made up of PVC and some from iron.

5.4 Managing the engineering information

The main engineering information and the characteristics of the water and sewer network are the diameter of the pipes, the material that are made of, the length of the pipes, the historical background of the leaks and other issues, the type of the pipes, the x-,y-coordinates, and z- where it was possible. The water and sewer supply network consists of pipes with many different diameters, but the majority of it is pipes with 90 cm diameter for the water system and 125 cm for the sewer system (figure 16). The figure 17 shows the depiction of the digitized sewer and network data in reality.

Figure 16: The pipe diameter of sewer network after the digitization.

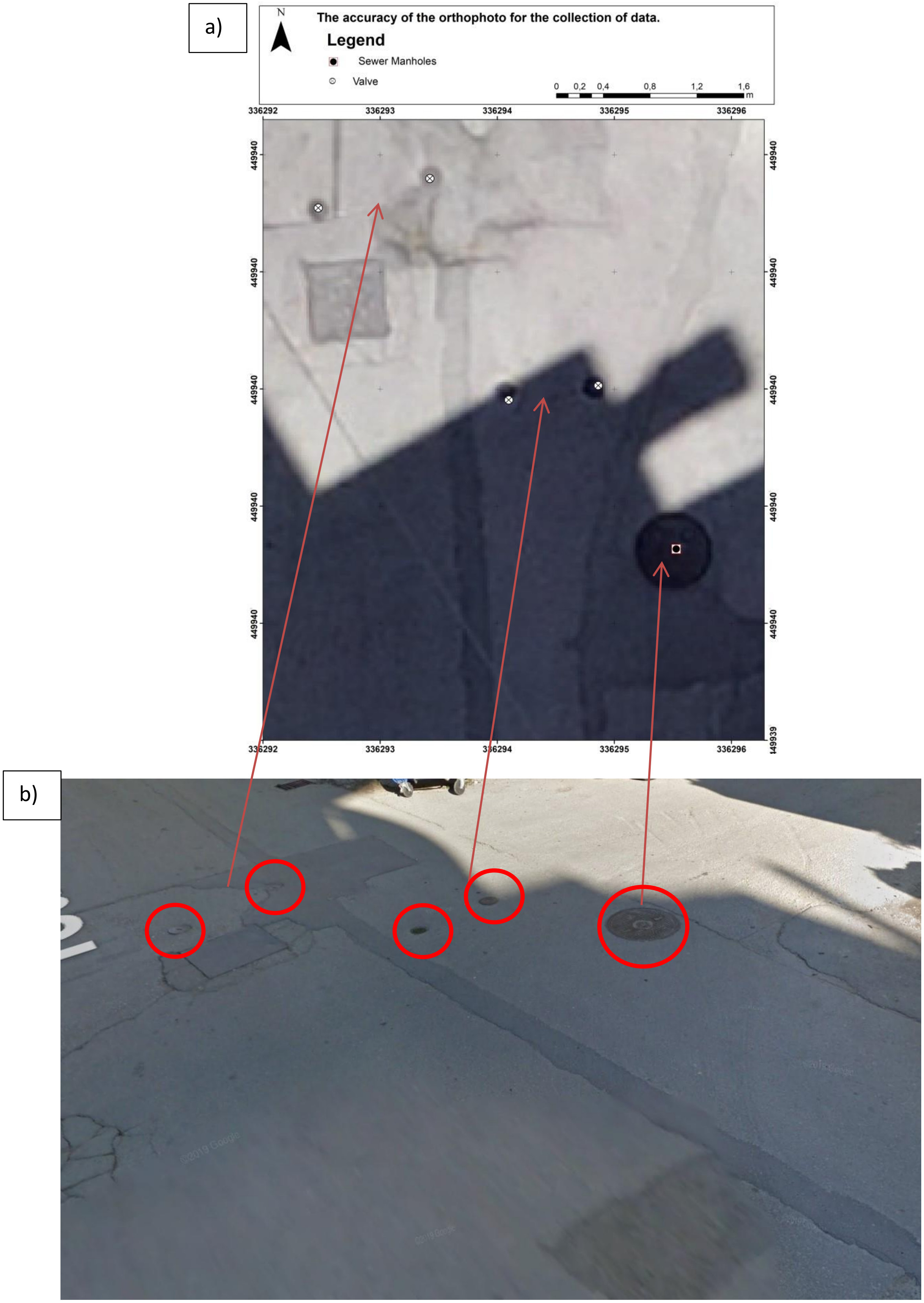

Figure 17: The visualization of the study area in a) GIS and b) in reality.

5.5 Spatial database

Through the development of the GIS for the water company, many and varying kinds of information are coming from various sources, stored in a variety of forms. A spatial database was created in order to solve this issue and to provide classified and organized information about the data. Specifically, 362 valves, 123 fire hydrants, 10850 water meters, 3580 consumer manholes, 360 wells, 961 sewer manholes, 3957 water network pipes and 1895 sewer network pipes were stored that are essential for the water company's GIS system. The following figure 18, figure 19 and figure 20 depict the data in maps.

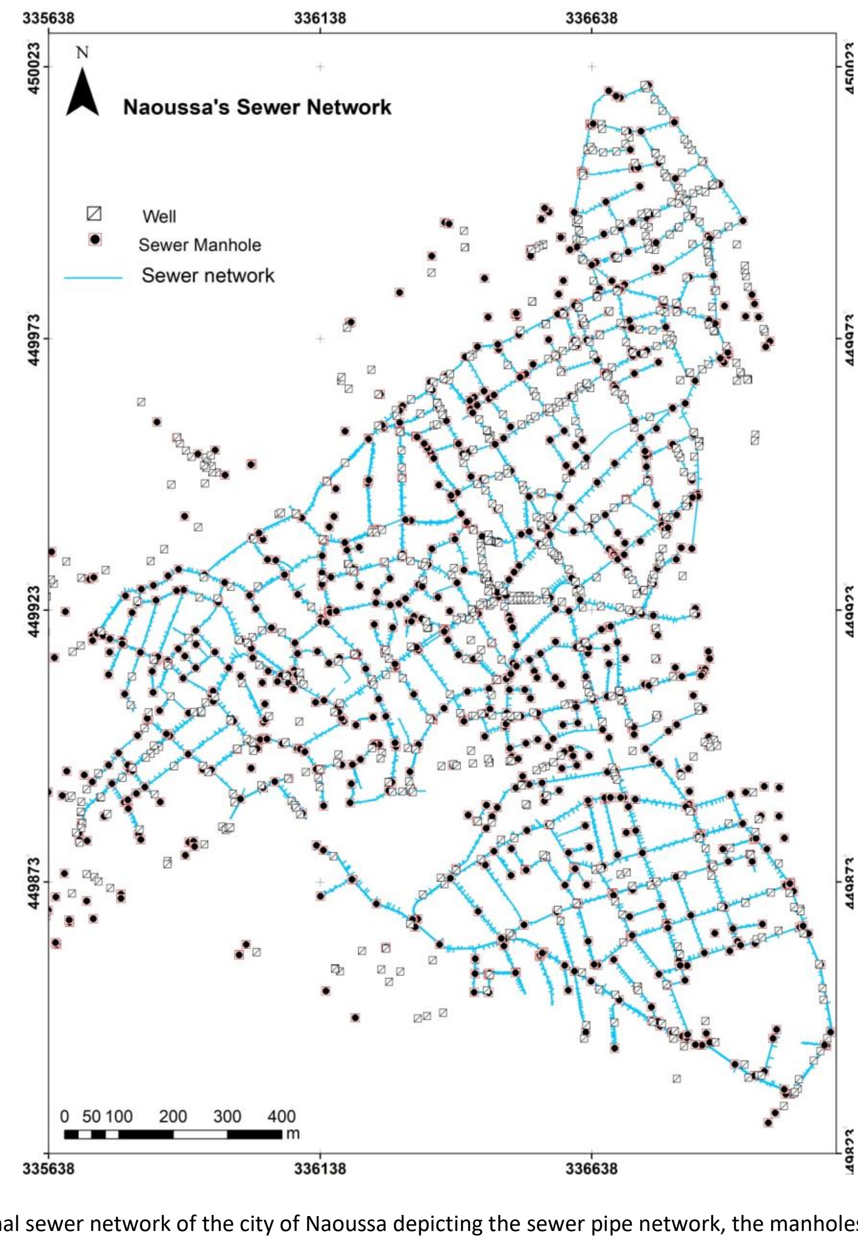

Figure 18: Final sewer network of the city of Naoussa depicting the sewer pipe network, the manholes and the wells.

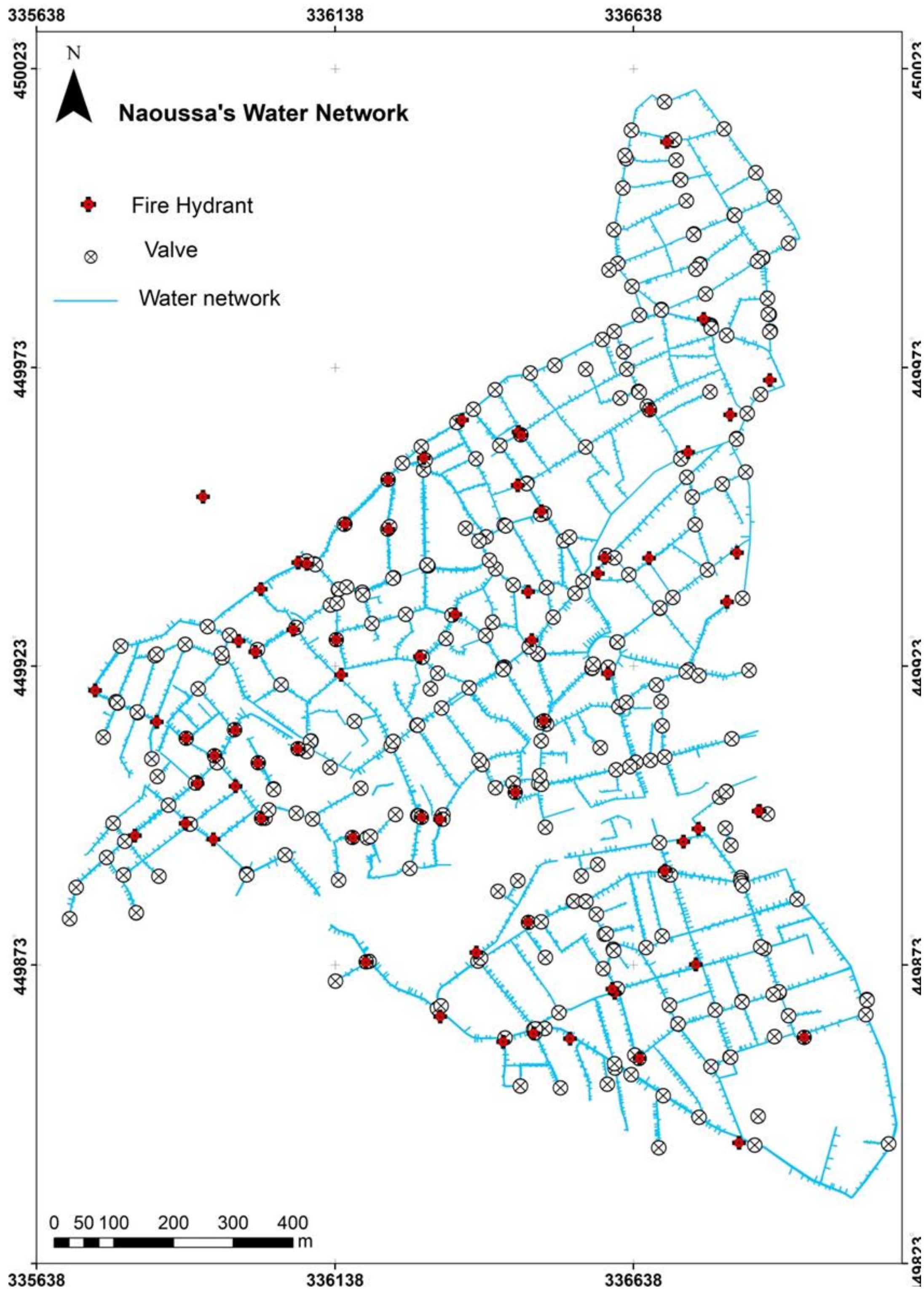

Figure 19: Final water network of the city of Naoussa depicting the water pipe network, the fire hydrants and the valves.

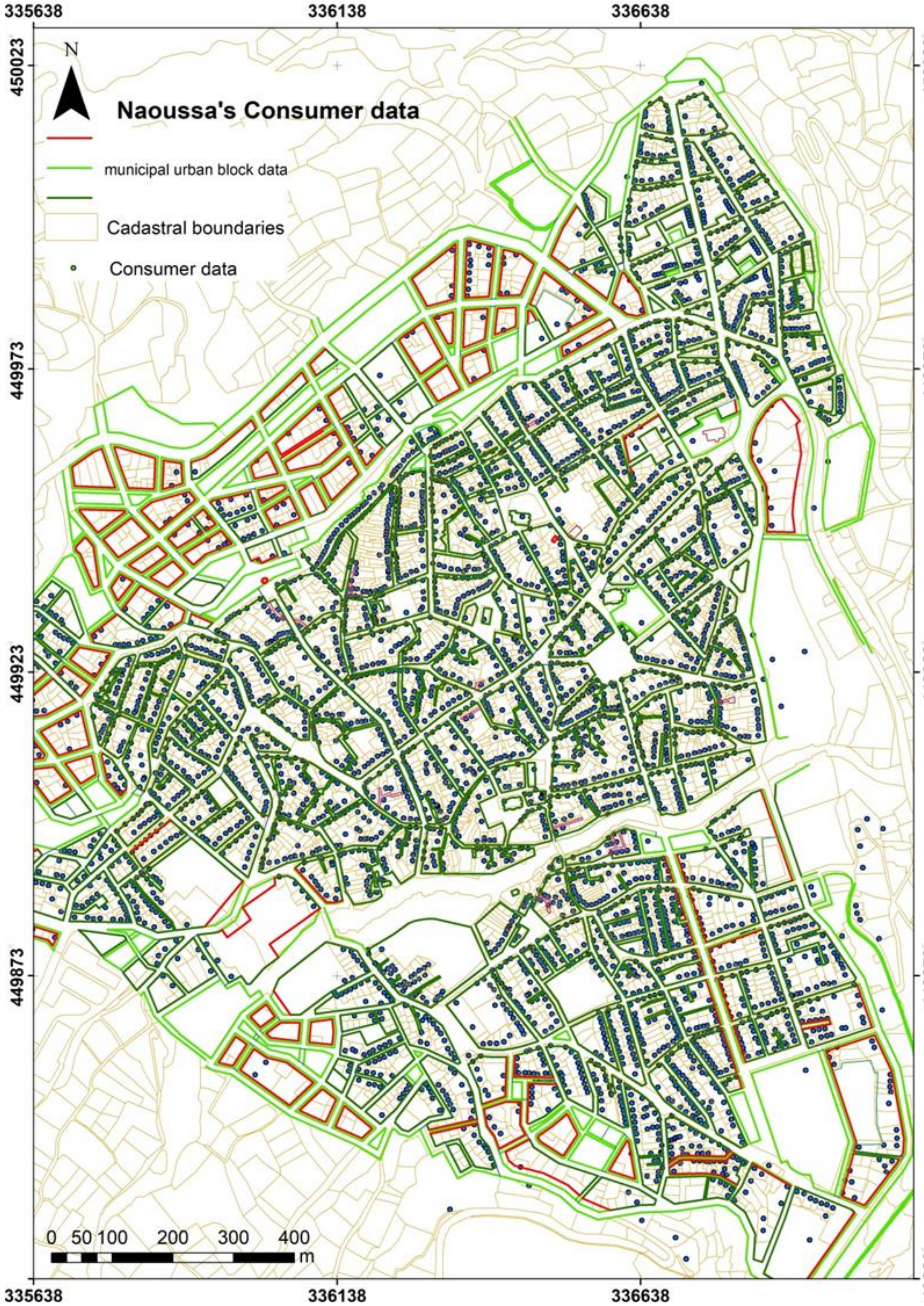

Figure 20: Final consumers data of the city of Naoussa with the water meter of each house and their property.

5.6 Indicative scenarios for management of the water distribution and sewage network

Three examples of applications for the constructed database were developed. The developed management scenarios were selected based on two criteria. The first criterion is the showing of useful network management capabilities, and the second is suitability of the created GIS system for the Water Company.

1st Scenario

In the first scenario, it is assumed that the water supply company wishes to introduce some new items into the water supply network that it deems necessary for its better operation. Of course, the introduction of new objects must not conflict with the rules of connection of the network objects selected. Thus, we must e.g. to connect pipeline to an existing transmission pipeline.

This process is completed through ArcMap. Initially, all pipeline layers are set as selectable layers from the set selectable layers option. Then the editing process starts having selected “create new feature” in the task menu. Also, in the target menu, the pipeline class is selected as the destination class of the new object. It is selected to snap the new object along the line of the distribution pipeline to which the new object have been connected. So the choice is snapping to distribution main edge. In the next step, the sketch tool is selected from the editor’s toolbar and with this the new object is inserted. As the pointer moves on the map it automatically snaps along distribution pipeline lines. Once the appropriate point is found, it is selected by clicking and from there the insertion of the new object begins. Right-clicking allows the perpendicular and length options to set the new object to be perpendicular to the distribution pipe and to be 45 m long, respectively. This creates a new distribution pipeline, which is perpendicular to the distribution pipe and is 45 m long.

By creating the new pipeline, it is established that the connection rules are respected by the geodatabase and both pipelines are joined by a Valve object. **Figure 21** shows the introduction of a distribution pipeline into the geometric network and its connection to a transmission pipeline.

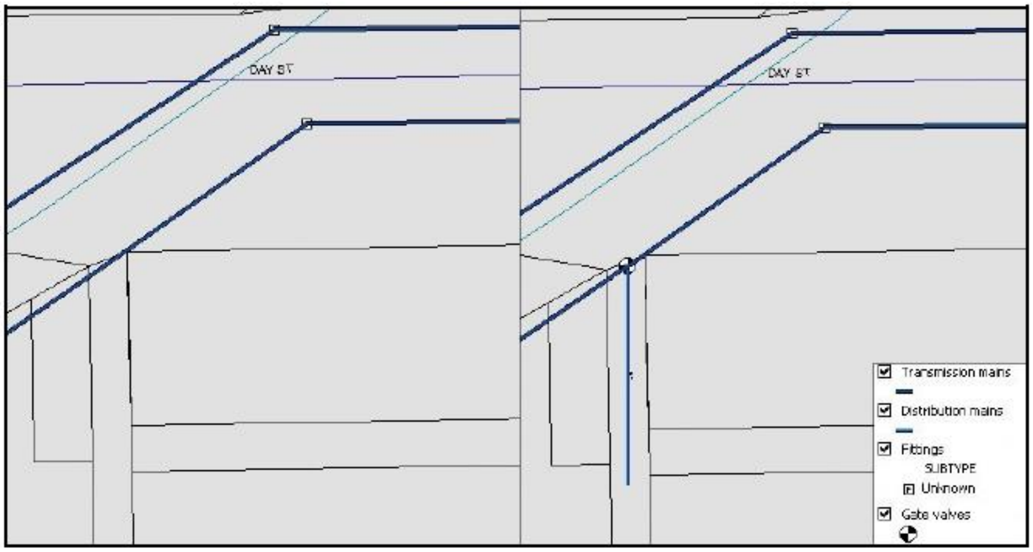

Figure 21: Insert of a new distribution pipe above in a transport pipeline in the geometric network.

2nd Scenario

In the second management scenario, the water company wishes to find the path of the connection between two pipelines in the network, which supply an important customer. This has to be done because some pipelines have to be closed due to replacement and it has to be determined if they affect the water supply on that particular route.

This scenario can be resolved through the analysis menu provided by the "network analyst toolbar utility" in ArcMap. Initially, from the flags/barriers button on the bar, the insert of two flags is selected, one for each of the two conductors whose connection path is of interest. Then the find path command is selected from the analysis menu and then the resolve button. As a result, ArcMap draws the connecting route between the two pipelines by (if there are alternative routes) the shortest distance. **Figure 22** shows the connection path between the two pipelines selected.

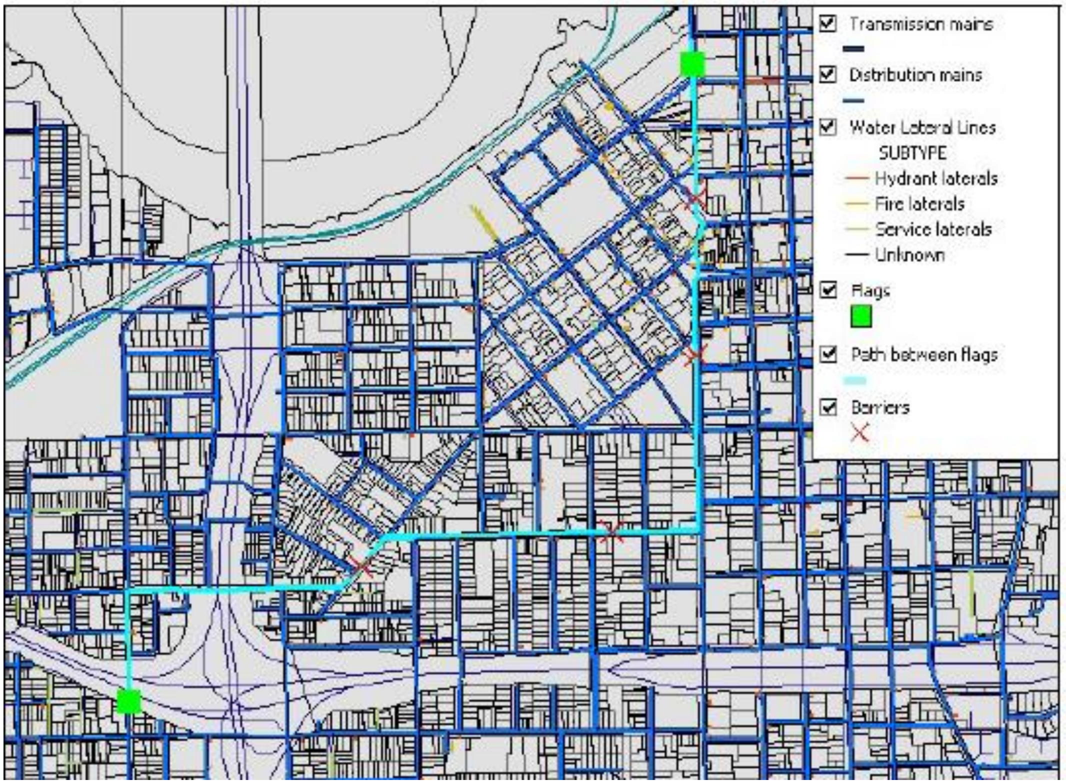

Figure 22: Find the path of the connection between two selected pipelines.

As can be seen from the **Figure 22**, barriers are then placed on the pipelines that must stop their operation due to replacement and at the same time they are on the critical path. Thus, the flags/barriers button places barriers on the selected pipelines. Finally, the solve button gives the new path that will connect the two pipelines, as shown in **Figure 23.**

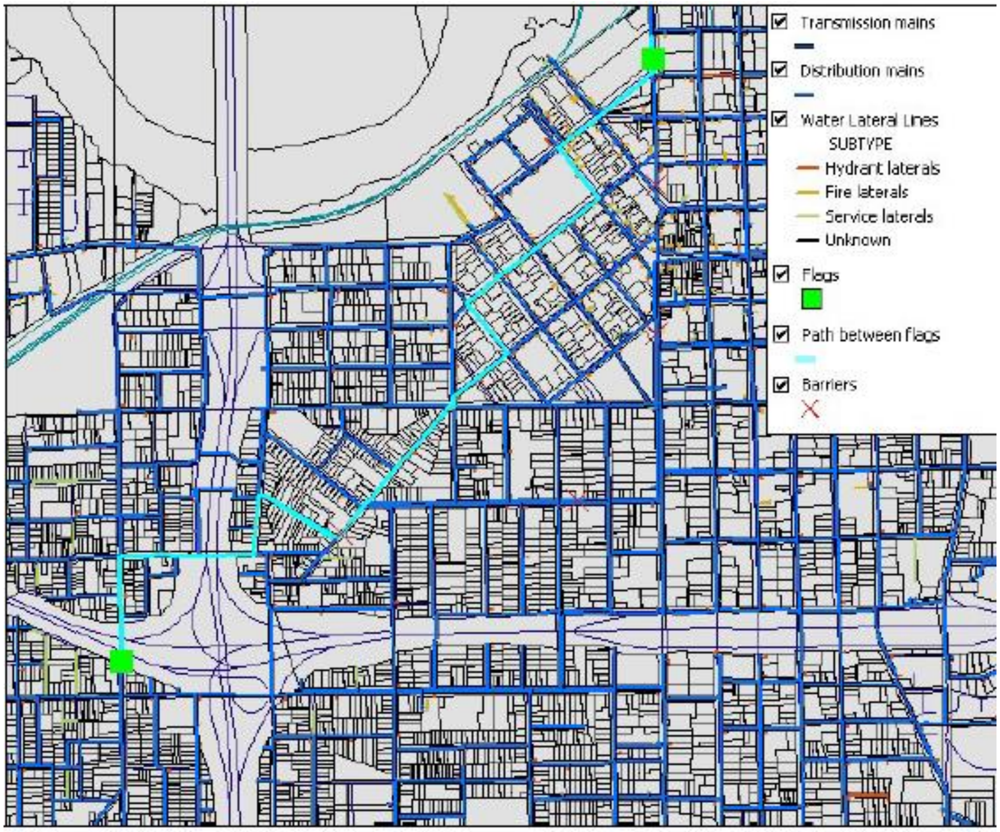

Figure 23: Finding the new path of the connection between two pipelines after entering obstacles along the old path.

3rd Scenario

The third network management scenario is again about network analytic capabilities. In this case, the water company wishes to isolate from the flow of water a distribution pipe of its network in which a leak has been observed. This can be done by finding the system valves that need to be closed to stop the flow of water in that particular pipe.

First, the appearance of the area in which the conductor to be isolated is located is selected. From the flags and barriers button of the network analyst toolbar, the insertion of a line flag is selected, which is then attached to the pipeline in question. Then, from the analysis menu of the bar, the disable layers command is selected and with this the system valves layer is disabled, so that its objects interrupt the network detection process. In the same menu and with the options command, a detection settings window opens. In the Results tab of this window, the results are chosen to be in the form of selected objects (and not a drawing) and to contain the objects in which the detection is stopped (features stopping the trace). Finally, from the trace task menu of the network analysis bar, the detection method find connected is selected, which finds all objects connected to the flagged point. In this case this point is the conductor that needs to be isolated. With the above options, it is essentially specified in ArcMap to select all those network objects that are disabled (i.e. system valves), and that are connected to the selected pipeline, but stopping the process of network detection from it to the rest of the network. More simply, all system valves are selected that if closed will stop the water supply to the flagged pipeline. The above proposition is confirmed by pressing the solve button of the network analysis toolbar and the result is shown in **Figure 24** below. Figure 24 shows the valves that must be closed (in blue) to cut off the water supply to the pipeline where the flag was placed (in green).

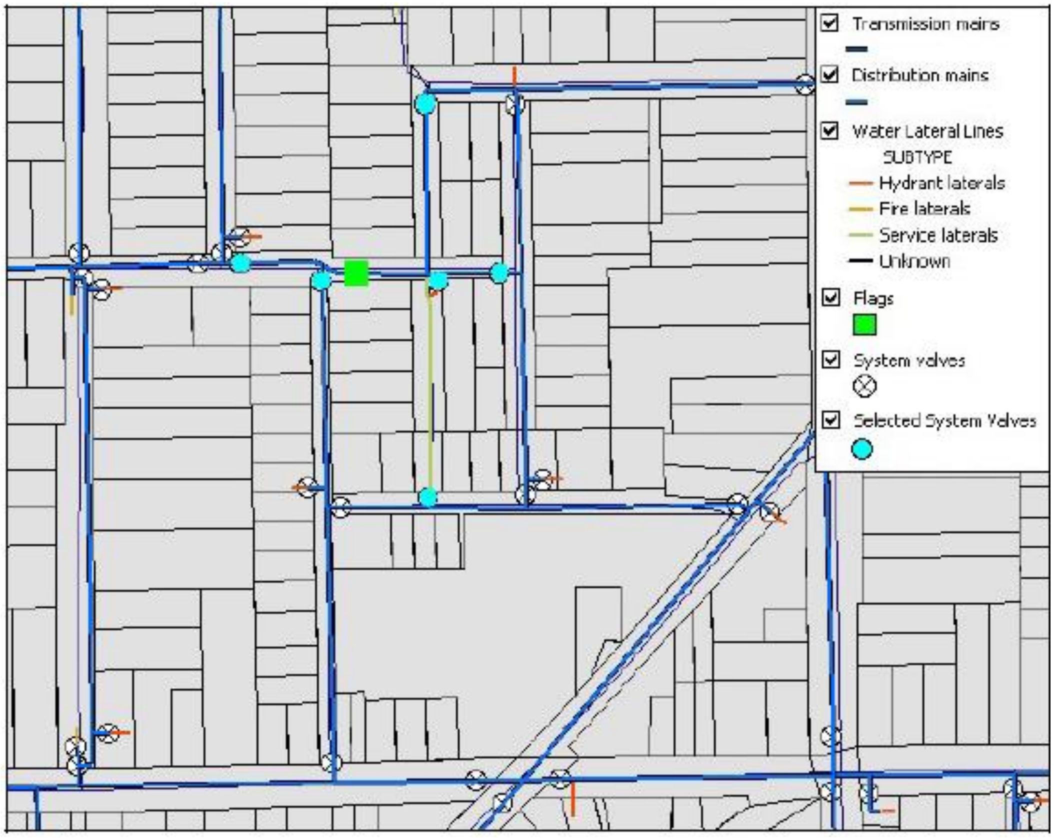

Figure 24: Find the system valves to shut off the water supply to the flagged mains pipe.

6. Discussion

This thesis showed how the GIS can help the water company in their everyday work. The implementation process used can provide other water companies with the methodology and knowledge to apply and develop their GIS system from the scratch.

From the interpretation of the previous maps we can draw some reasonable conclusions about the water supply network of Naoussa, and the possibility of an appropriately designed GIS for its management. As suggested by Reger, (2017) and Mickrenska, (2020), GIS can provide the utility a water agency needs, with endless information about their assets, spatial and non-spatial.

In the application made in Naoussa, 58 flights were carried out. A total of 21000 photographs were taken covering the area of Naoussa. The data of the nadir images were used for the production of the orthophoto map.

To check the accuracy of the orthophoto, 85 points whose geodetic coordinates were known were used and the same points were planned in the model. By using 85 GCPs, the accuracy of the final orthophoto was 4.5cm and produced using the Agisoft Metashape. Accuracies between the range of 4.5 – 10 cm was achieved by Chen et al., (2008); Anurogo et al., (2017); Tsouros (2019); and Sokratis, (2019), by using the photogrammetric method for the production of the orthophoto.

However, if greater accuracy is desired, these coordinates should be corrected by further targeting the point on the photos in the editing software, or aiming at the photos from the beginning.

For the comparison of the two mapping methods, the differences of 15.21 cm, 16.14 cm and 16.8 cm for X-, Y- and Z- coordinates from the ground survey method provides a closer planimetric result compared to 26.6 cm, 29.87 cm and 29.32 cm from the photogrammetric method respectively.

Eyoh et al. (2019) also found that the ground survey method gives closer and more accurate results compared with those produced by the photogrammetric method. They calculated the horizontal accuracy of the survey method to be 23 cm, as compared with 25 cm accuracy from the UAV method.

Regarding the utility of the photogrammetric application, comparing field and office work times it is understood that it saves mainly time but also money for the Company. In contrast to the ground survey method, by staying in the field to obtain the primary data takes days while the office work takes also many days. In contrast, for the creation of an orthophoto with terrestrial geodetic methods, the field work and rendering of the plan can take up to a week.

However, one can work in addition to the other. With the total station, the engineer can record everything in the field of view of the instrument. With the drone, all the details of a building can be photographed except for those hidden behind other natural objects such as trees.

With the first scenario, the preservation of data integrity was shown thanks to subtypes and value-defining fields and the application of binding rules when inserting new objects into the network. With the second and third scenarios, the unlimited analysis capabilities (flow determination and network tracing) provided by a GIS system for a water supply network were shown.

The amount of information that was used in the creation of geographic information system for the water network was large. The greater the final number of elements used, the more complex the organization of database becomes. The organization of database and the creation of geographic information system to meet the needs of the Company was based on the study carried out for the Municipal Water Supply and Sewerage Company of Chania L, (1995). The cartographic background fields proposed in the application were, valves, fire hydrants, water meters, consumer manholes, wells, sewer manholes, water network pipes and sewer network pipes. More specifically, the databases included data concerning the geometric position of each element as well as non-descriptive, non-geometric characteristics.

6.1 Limitations

The limitations encountered led several times to the revision of the performed procedures and work flows. More problems were encountered during office work than during field work.

Regarding some difficulties in the fieldwork, a major issue was the wind. Sudden gusts of air can disrupt the stable flight path of the flying vehicle, resulting in some distortion or blurring of the photos and the possibility of incorporating incorrect coordinates into the image. These will contribute to a worse than ideal point matching and subsequently to a less accurate optimization of camera positions in space. But this does not necessarily mean that the accuracy of the model will decrease. The reason mentioned is because it might affect the appearance factor.

Areas with dense vegetation present difficulties and delays in the point densification stage. This is because trees and plants have a strange geometry. The solutions to this problem are either to produce a lower quality dense cloud or to generalize more strongly on it.

Most problems were identified at the stage of processing and production of the final orthophoto. These stem mainly from the limited computing power available to the computer used for processing. Agisoft Metashape software demands powerful CPU and GPU processing, which can strongly decrease the computational time process. In this way the hardware that is needed for this kind of process must be very capable.

The difficulty encountered is that during the alignment, process was 50% complete after 48 hours of continuous processing. This was due to both the limited capabilities of the system and the excessively large number of photographs, many of which had both common views and large overlaps.

Also, the data collected by the drone achieve very good horizontal and height accuracy, for example 4.5 cm of the final orthophoto map. Accuracy could be better if the flight height was lower, as found by other studies.

6.2 Future implementation

The modeling of a water supply network that will include special SCADA sensors, to provide real-time network data, makes possible the creation of a real-time network management system with network leakage and fault management capabilities.

Another future implementation is the development of a Web based GIS application, so all employees can have access online without the use of specific GIS software in their computer.

7. Conclusion

By focusing on the development of a GIS for Water Company, this thesis explored the design and implementation of a GIS for the Naoussa Municipality Water and Sewer Company for better water utility management. Moreover, the more accurate way of mapping for water and sewer data collection was investigated.

Considering the 3 scenarios for the better management of the water and sewer network, they showed the possibilities of adapting the model when introducing new objects into the water supply network, but also the possibilities of correct data entry using subtypes and value definition fields. Solving realistic scenarios makes clear the possibilities of network probing and executing "what if" scenarios that can solve various problems that are likely to arise when managing a complex network such as a water distribution network.

From the comparison of the two mapping methods, the ground survey method proved to be more accurate than the UAV photogrammetry technique. However, with respect to the degree of detail, the method of photogrammetry provides a much better description of the area excels in survey speed, the cost of data collection, as well as the ease with which it can be the whole work is carried out, especially when it comes to difficult or hard to reach areas.

Approximately, 22000 field data collected (like valves, sewer manholes, hydrometers, hydrants, pipelines, storm water manholes and wells) and stored in a spatial database along with their engineering information. Now the Water Company knows exactly where everything is and its condition since everything was unknown.

The final implementation of the GIS for the Water Company provided the necessary tools for the production of maps, ensured valid and complete knowledge of the networks, gave access to all the departments, and the senior executives of the company who make use of this information for strategic planning. Also, requests from the customers can be easily located by the employees in the office instead of searching the field.

8. References

Anurogo, W. et al. (2017). A Simple Aerial Photogrammetric Mapping System Overview and Image Acquisition Using Unmanned Aerial Vehicles (UAVs). Journal of Applied Geospatial Information . 01. 11-18. 10.30871/jagi.v1i01.360.

Cannistra, J.R. (1999), Converting utility data for a GIS. Journal - American Water Works Association, 91: 55-64. https://doi.org/10.1002/j.1551-8833.1999.tb08585.x

Toreti et al.(2022), Drought in Europe. Publications Office of the European Union, Luxemburg, 2022, ISBN 978-92-76-54953-6 (online), doi: 10.2760/014884 (online), JRC130253.

Crawford, D., & Hung, M. (2012). Implementing a Utility Geographic Information System for Water, Sewer, and Electric: Case Study of City of Calhoun, Georgia. Urisa Journal, 26, 25.

Tsouros, Dimosthenis C., Stamatia Bibi, and Panagiotis G. Sarigiannidis. 2019. "A Review on UAV-Based Applications for Precision Agriculture" Information 10, no. 11: 349. https://doi.org/10.3390/info10110349

ESRI (2016) *Implementing ArcGIS for Water Utilities*. California: ESRI.

Eyoh, A., Ubom, O. and Ekpa, A. (2019) 'Comparative analysis of UAV photogrammetry and total station traversing on route survey', *European Journal of Engineering and Technology*, 7(4), pp. 60–72.

Fellers J. (2013), "Implementing a Geographic Information System for a Rural Water and Sewer Company: A Case Study of the Newberry County Water and Sewer Authority". Northwest Missouri StateUniversity Maryville, Missouri

Gashi, F. *et al.* (2018) 'Application of GIS in the water company " HIDRODRINI " - PEJË', in Bandrova T., K. M. (ed.) *7th International Conference on Cartography and GIS*. Sozopol, Bulgaria, pp. 18–23.

Huber, M. (2021) *An automated unmanned aerial vehicle – structure from motion pipeline to create analysis-ready digital surface models for coastal monitoring*. Lund University. http://lup.lub.lu.se/student-papers/record/9066921

Lates, I. *et al.* (2018) 'Applications of gis model for water supply systems', *Land Reclamation, Earth Observation & Surveying, Environmental Engineering*, VII, pp. 146–151.

Iustina, Lates & Luca, Mihail & Ilie, Gelu & Dumitrascu, Nicoleta. (2016). Studies on the Implementation of GIS Model in Water Supply Systems. Present Environment and Sustainable Development. 10. 10.1515/pesd-2016-0033..

Lyon, T. and Clifford, D., 2008. From deficient to efficient many benefits flow from water district's GIS [Online]. ArcUser Online, Spring. Available from: http://www.esri.com/news/arcuser/0708/metamorphosis.html

Maidment, D. R., & Morehouse, S. (2002). Arc Hydro: GIS for water resources. ESRI, Inc.

Marinaki M. and Papageorgiou M. (1997), “Central Flow Control in Sewer Networks”. Journal of Water Resources Planning and Management, (123), 274-283.

Mickrenska-Cherneva, & Mladenov, R. . (2020). Implementation of GIS Application for Water Company Needs. Geomatics and Environmental Engineering, 14(4), 47–56. https://doi.org/10.7494/geom.2020.14.4.47

Municipality of Naoussa (2023), retrieved from https://www.naoussa.gr/en/

Municipal Water Supply and Sewerage Company of Chania (1995), water supply in the area of Chania", Chania

Patil J. A. (2014), "Design and Mapping of Underground Sewerage Network in GIS-A Case Study". International Journal of Science and Research (IJSR), Volume 3, Issue 8, pp 424-431.

Petroulias, N., Foufeas, D., & Bougoulia, E. (2016). Estimating water losses and assessing network management intervention scenarios: the case study of the water utility of the city of Drama in Greece. Procedia engineering, 162, 559-567.

Rayburn, S. R. 2004. The Use of GIS in Water Utility Asset Management, Four Seasons Subdivision of Lufkin, Texas. Master’s Thesis. Stephen F. Austin State University.

Reger C.M. Master’s Thesis. University of Southern California; Los Angeles, CA, USA: 2017. Bringing GIS to a Small Community Water System. Availableonline:http://digitallibrary.usc.edu/cdm/ref/collection/p15799coll40/id/330742 [Google Scholar]

Shamsi, U. M. (2005). GIS applications for water, wastewater, and stormwater systems. CRC press.

Sokratis, M. (2019) *The accuracy in surveying with unmanned aircraft system (UAS)*. (Master's Thesis, Aristotle University).

Vega, R. (2009). Managing Water Utilities with Geographic Information Systems: The Case of the City of Tampa, Florida: a Thesis Presented to the Department of Geology and Geography in Candidacy for the Degree of Master of Science (Doctoral dissertation, Northwest Missouri State University).

Wang, Z., Wei, Z., & Yin, Q. (2008). The design of water supply network based on GIS. 2008 IEEE Conference on Cybernetics and Intelligent Systems, 209-213.

Yan, B., Su, X. and Chen, Y. (2008) 'Data Management of Urban Water Supply Network Based on GIS', in *ISECS International Colloquium on Computing, Communication, Control, and Management 2008 ISECS International Colloquium on Computing, Communication, Control, and Management Data*. IEEE, pp. 358–362. doi: 10.1109/CCCM.2008.370.

Newsbeast 2018, *The waters of Naoussa*, Retrieved January 19,2021, from www.newsbeast.gr/travel/arthro/3370058/i-entiposiaki-katarraktes-tis-naousas

Zhao, Y. W., Qin, Y. (2009). "GIS-based optimization for the locations of sewage treatment plants and sewage outfalls – A case study of Nansha District in Guangzhou City, China". Communications in Nonlinear Science and Numerical Simulation, (14), 1746-1757.

Appendix A

Appendix A – SCADA telemetry meters for future potential installation.

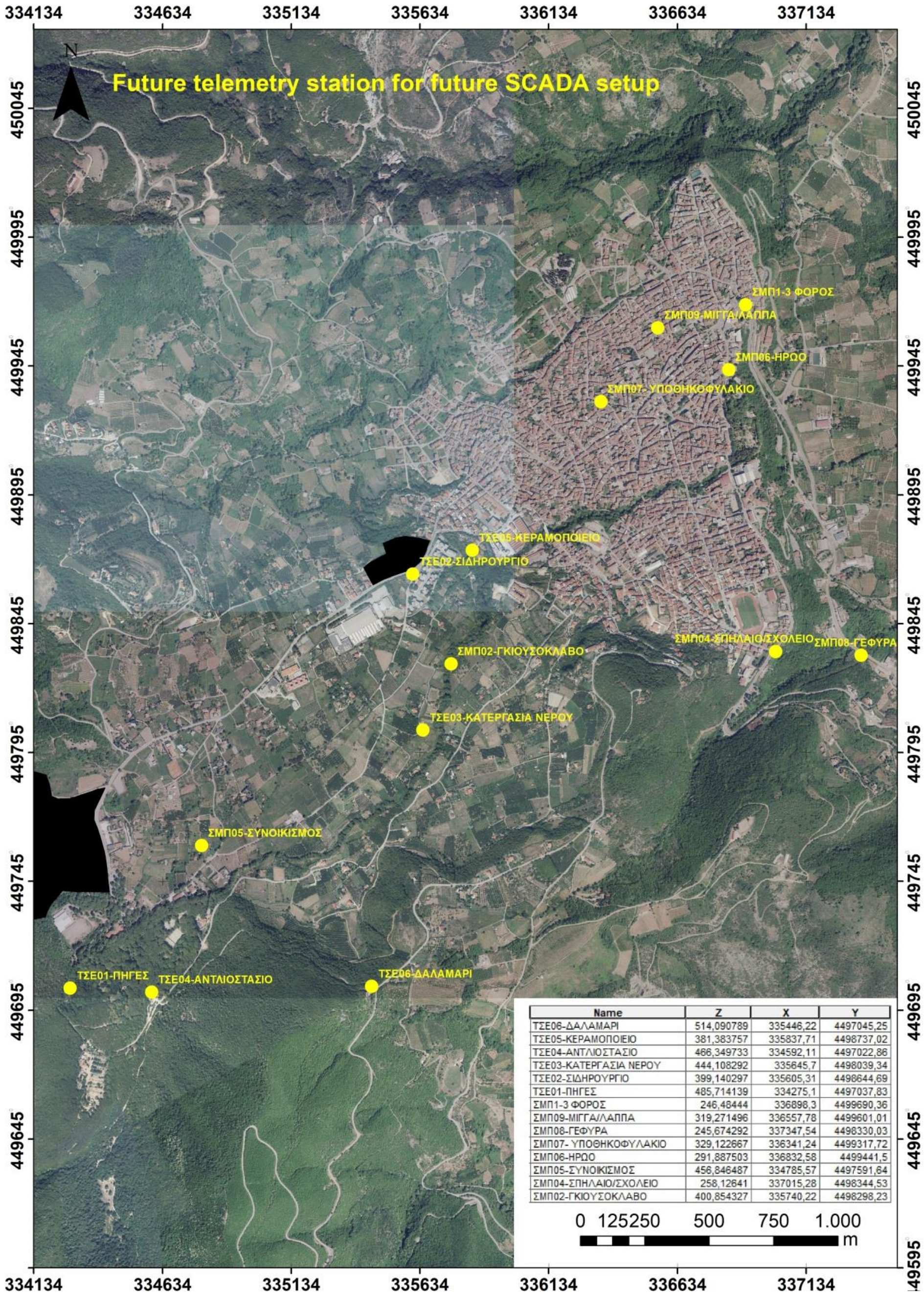

Appendix B

Appendix B – Reference coordinates of GCPs for accuracy check.

Label	Reference Coordinates		
	X(m)	Y(m)	Z(m)
GCP 1	336249.25	4499627.25	327.60
GCP 2	336253.97	4499626.96	328.39
GCP 3	336370.47	4499661.33	327.79
GCP 4	336373.88	4499658.89	327.81
GCP 5	336338.64	4499633.98	330.22
GCP 6	336344.53	4499634.99	329.80
GCP 7	336355.28	4499604.61	331.78
GCP 8	336361.14	4499604.15	331.55
GCP 9	336284.54	4499575.35	336.37
GCP 10	336286.37	4499575.72	336.40
GCP 11	336288.08	4499557.42	336.69
GCP 12	336289.47	4499558.79	336.50
GCP 13	336288.54	4499474.04	337.77
GCP 14	336292.86	4499475.46	337.68
GCP 15	336239.33	4499374.60	344.64
GCP 16	336238.65	4499375.27	344.56
GCP 17	336183.76	4499354.45	349.12
GCP 18	336186.08	4499356.39	348.82
GCP 19	336210.50	4499345.20	347.82
GCP 20	336213.36	4499344.53	347.63
GCP 21	336201.17	4499302.67	349.38
GCP 22	336201.96	4499301.39	349.49
GCP 23	336256.37	4499317.62	346.55
GCP 24	336260.10	4499318.37	346.23
GCP 25	336289.31	4499327.62	344.73
GCP 26	336296.43	4499329.46	344.52
GCP 27	336336.75	4499313.83	345.92
GCP 28	336338.57	4499315.57	345.92
GCP 29	336354.84	4499253.69	346.15
GCP 30	336356.69	4499256.55	346.01
GCP 31	336419.77	4499227.02	343.93
GCP 32	336422.06	4499226.66	343.65
GCP 33	336426.00	4499224.26	343.31
GCP 34	336427.58	4499226.37	343.30
GCP 35	336365.85	4499192.76	345.37

GCP 36	336367.65	4499193.34	345.11
GCP 37	336396.43	4499146.60	345.70
GCP 38	336397.46	4499149.52	345.65
GCP 39	336492.94	4499132.92	343.21
GCP 40	336494.94	4499135.71	343.04
GCP 41	336522.45	4499139.50	341.82
GCP 42	336524.49	4499140.77	341.66
GCP 43	336613.82	4499164.06	338.80
GCP 44	336612.08	4499165.89	338.82
GCP 45	336622.82	4499171.24	338.48
GCP 46	336624.88	4499171.47	338.24
GCP 47	336673.02	4499200.69	336.17
GCP 48	336672.46	4499201.74	336.07
GCP 49	336747.12	4499219.87	335.55
GCP 50	336751.42	4499220.31	335.54
GCP 51	336831.45	4499222.12	334.42
GCP 52	336831.85	4499223.19	334.33
GCP 53	336842.71	4499114.18	332.66
GCP 54	336841.63	4499113.56	332.74
GCP 55	336824.93	4499073.00	332.76
GCP 56	336824.97	4499075.11	332.90
GCP 57	336762.00	4499391.01	330.43
GCP 58	336760.78	4499390.92	330.50
GCP 59	336816.96	4499430.14	327.79
GCP 60	336817.16	4499430.79	327.78
GCP 61	336833.05	4499437.82	326.94
GCP 62	336833.68	4499439.13	326.70
GCP 63	336823.10	4499437.54	327.50
GCP 64	336823.45	4499438.00	327.32
GCP 65	336560.13	4499370.95	334.31
GCP 66	336561.54	4499372.15	334.25
GCP 67	336508.18	4499369.47	336.48
GCP 68	336509.82	4499372.51	336.30
GCP 69	336492.69	4499361.65	337.44
GCP 70	336494.52	4499362.36	337.42
GCP 71	336436.39	4499365.76	340.24
GCP 72	336438.58	4499369.62	339.97
GCP 73	336397.42	4499407.57	339.52
GCP 74	336399.56	4499409.81	339.14
GCP 75	336432.85	4499469.81	334.65
GCP 76	336436.94	4499471.02	334.52

GCP 77	336415.68	4499476.22	334.93
GCP 78	336417.38	4499479.92	334.97
GCP 79	336460.35	4499535.28	331.98
GCP 80	336463.72	4499537.10	331.62
GCP 81	336406.63	4499518.00	333.75
GCP 82	336404.60	4499519.13	333.92
GCP 83	336648.28	4499465.26	330.11
GCP 84	336650.67	4499467.10	330.00
GCP 85	336628.72	4499510.49	329.32

Appendix C

Appendix C – Results of Total Station and UAV Coordinates of GCPs.

Label	**Total Station**			**UAV Photogrammetry**		
	X(m)	**Y(m)**	**Z(m)**	**X(m)**	**Y(m)**	**Z(m)**
GCP 1	336249.17	4499627.35	327.10	336249.25	4499627.25	327.60
GCP 2	336253.99	4499627.19	328.58	336254.23	4499627.20	328.78
GCP 3	336370.49	4499661.47	327.92	336370.50	4499661.65	328.03
GCP 4	336373.94	4499659.02	328.01	336374.14	4499659.23	328.16
GCP 5	336338.78	4499634.09	330.28	336338.87	4499634.26	330.35
GCP 6	336344.60	4499635.01	329.85	336344.79	4499635.15	329.95
GCP 7	336355.35	4499604.65	331.87	336355.39	4499604.79	332.04
GCP 8	336361.29	4499604.38	331.62	336361.32	4499604.57	331.79
GCP 9	336284.76	4499575.47	336.56	336284.82	4499575.55	336.80
GCP 10	336286.58	4499575.83	336.51	336286.78	4499575.95	336.62
GCP 11	336288.17	4499557.58	336.72	336288.32	4499557.65	336.76
GCP 12	336289.72	4499558.82	336.68	336289.83	4499558.83	336.73
GCP 13	336288.72	4499474.29	337.93	336288.73	4499474.44	338.07
GCP 14	336292.87	4499475.60	337.84	336292.89	4499475.72	337.90
GCP 15	336239.46	4499374.86	344.78	336239.71	4499374.95	345.04
GCP 16	336238.69	4499375.46	344.81	336238.83	4499375.64	344.90
GCP 17	336183.81	4499354.63	349.23	336183.85	4499354.85	349.47
GCP 18	336186.15	4499356.65	348.98	336186.40	4499356.66	348.99
GCP 19	336210.59	4499345.26	347.83	336210.80	4499345.30	347.88
GCP 20	336213.41	4499344.66	347.68	336213.50	4499344.70	347.81
GCP 21	336201.41	4499302.93	349.54	336201.51	4499303.03	349.67
GCP 22	336202.18	4499301.53	349.55	336202.29	4499301.59	349.78
GCP 23	336256.58	4499317.67	346.58	336256.76	4499317.81	346.65
GCP 24	336260.21	4499318.60	346.40	336260.27	4499318.68	346.48

GCP 25	336289.52	4499327.75	344.75	336289.78	4499327.81	344.94
GCP 26	336296.65	4499329.61	344.62	336296.69	4499329.74	344.85
GCP 27	336337.01	4499313.99	346.10	336337.17	4499314.03	346.21
GCP 28	336338.79	4499315.65	346.01	336338.89	4499315.80	346.04
GCP 29	336354.96	4499253.79	346.24	336355.16	4499254.03	346.29
GCP 30	336356.82	4499256.80	346.16	336357.01	4499256.95	346.28
GCP 31	336419.83	4499227.09	344.01	336420.06	4499227.19	344.16
GCP 32	336422.29	4499226.91	343.85	336422.55	4499227.01	343.89
GCP 33	336426.18	4499224.44	343.53	336426.35	4499224.68	343.68
GCP 34	336427.84	4499226.48	343.46	336427.85	4499226.65	343.68
GCP 35	336366.01	4499192.85	345.39	336366.17	4499193.10	345.65
GCP 36	336367.68	4499193.57	345.35	336367.87	4499193.58	345.45
GCP 37	336396.46	4499146.86	345.86	336396.72	4499147.12	346.08
GCP 38	336397.65	4499149.75	345.75	336397.76	4499149.86	345.78
GCP 39	336493.03	4499133.04	343.24	336493.21	4499133.05	343.34
GCP 40	336495.00	4499135.88	343.07	336495.06	4499136.01	343.30
GCP 41	336522.53	4499139.74	341.92	336522.60	4499139.99	342.06
GCP 42	336524.59	4499140.98	341.78	336524.79	4499141.01	342.03
GCP 43	336613.89	4499164.12	339.03	336613.93	4499164.15	339.24
GCP 44	336612.34	4499165.99	339.02	336612.47	4499166.12	339.24
GCP 45	336622.94	4499171.46	338.57	336623.03	4499171.47	338.81
GCP 46	336625.12	4499171.50	338.47	336625.20	4499171.74	338.48
GCP 47	336673.11	4499200.93	336.33	336673.27	4499201.13	336.39
GCP 48	336672.64	4499201.90	336.31	336672.81	4499202.12	336.48
GCP 49	336747.16	4499220.05	335.67	336747.24	4499220.31	335.87
GCP 50	336751.45	4499220.39	335.64	336751.65	4499220.45	335.72
GCP 51	336831.70	4499222.26	334.55	336831.79	4499222.48	334.59
GCP 52	336831.86	4499223.44	334.53	336832.00	4499223.61	334.61
GCP 53	336842.83	4499114.19	332.90	336843.05	4499114.35	333.10
GCP 54	336841.81	4499113.74	332.91	336841.86	4499113.96	332.94
GCP 55	336824.98	4499073.10	333.01	336825.01	4499073.28	333.27
GCP 56	336825.00	4499075.32	332.95	336825.03	4499075.50	332.97
GCP 57	336762.15	4499391.19	330.64	336762.21	4499391.35	330.72
GCP 58	336760.95	4499390.97	330.62	336760.99	4499391.12	330.88
GCP 59	336817.18	4499430.32	327.97	336817.36	4499430.58	328.19
GCP 60	336817.30	4499431.03	327.94	336817.38	4499431.06	328.08
GCP 61	336833.24	4499437.91	327.05	336833.33	4499438.05	327.20
GCP 62	336833.88	4499439.39	326.96	336833.92	4499439.43	327.08
GCP 63	336823.21	4499437.55	327.54	336823.32	4499437.59	327.74
GCP 64	336823.63	4499438.02	327.51	336823.74	4499438.10	327.54
GCP 65	336560.36	4499371.16	334.51	336560.45	4499371.42	334.62

GCP 66	336561.70	4499372.22	334.44	336561.72	4499372.35	334.70
GCP 67	336508.41	4499369.68	336.66	336508.43	4499369.74	336.78
GCP 68	336509.92	4499372.53	336.49	336510.08	4499372.79	336.56
GCP 69	336492.87	4499361.66	337.63	336492.89	4499361.89	337.88
GCP 70	336494.70	4499362.39	337.53	336494.79	4499362.48	337.73
GCP 71	336436.56	4499365.98	340.27	336436.70	4499366.05	340.48
GCP 72	336438.69	4499369.84	340.06	336438.70	4499370.02	340.08
GCP 73	336397.46	4499407.60	339.78	336397.60	4499407.82	339.80
GCP 74	336399.59	4499410.07	339.40	336399.71	4499410.22	339.58
GCP 75	336433.00	4499469.91	334.89	336433.04	4499470.16	335.03
GCP 76	336437.13	4499471.03	334.75	336437.26	4499471.23	335.01
GCP 77	336415.83	4499476.26	335.17	336415.92	4499476.41	335.21
GCP 78	336417.57	4499480.00	335.01	336417.64	4499480.03	335.10
GCP 79	336460.40	4499535.48	331.99	336460.59	4499535.65	332.00
GCP 80	336463.93	4499537.23	331.86	336463.94	4499537.45	331.87
GCP 81	336406.80	4499518.07	333.96	336406.87	4499518.09	334.07
GCP 82	336404.77	4499519.26	333.97	336404.88	4499519.47	334.11
GCP 83	336648.33	4499465.46	330.21	336648.50	4499465.49	330.37
GCP 84	336650.73	4499467.18	330.12	336650.77	4499467.40	330.19
GCP 85	336628.79	4499510.57	329.57	336629.00	4499510.81	329.70

Appendix D

Appendix D – Differences in coordinate values from the referenced coordinates.

Label	**Reference-TST**			**Reference-UAV**		
	ΔE(m)	**ΔN(m)**	**ΔH(m)**	**ΔE(m)**	**ΔN(m)**	**ΔH(m)**
GCP 1	0.08	0.10	0.50	0.08	0.11	0.13
GCP 2	0.02	0.23	0.19	0.26	0.24	0.39
GCP 3	0.02	0.14	0.13	0.03	0.32	0.24
GCP 4	0.06	0.13	0.20	0.26	0.34	0.35
GCP 5	0.14	0.11	0.06	0.23	0.28	0.13
GCP 6	0.07	0.02	0.05	0.26	0.16	0.15
GCP 7	0.07	0.04	0.09	0.11	0.18	0.26
GCP 8	0.15	0.23	0.07	0.18	0.42	0.24
GCP 9	0.22	0.12	0.19	0.28	0.20	0.43
GCP 10	0.21	0.11	0.11	0.41	0.23	0.22
GCP 11	0.09	0.16	0.03	0.24	0.23	0.07
GCP 12	0.25	0.03	0.18	0.36	0.04	0.23
GCP 13	0.18	0.25	0.16	0.19	0.40	0.30
GCP 14	0.01	0.14	0.16	0.03	0.26	0.22

GCP 15	0.13	0.26	0.14	0.38	0.35	0.40
GCP 16	0.04	0.19	0.25	0.18	0.37	0.34
GCP 17	0.05	0.18	0.11	0.09	0.40	0.35
GCP 18	0.07	0.26	0.16	0.32	0.27	0.17
GCP 19	0.09	0.06	0.01	0.30	0.10	0.06
GCP 20	0.05	0.13	0.05	0.14	0.17	0.18
GCP 21	0.24	0.26	0.16	0.34	0.36	0.29
GCP 22	0.22	0.14	0.06	0.33	0.20	0.29
GCP 23	0.21	0.05	0.03	0.39	0.19	0.10
GCP 24	0.11	0.23	0.17	0.17	0.31	0.25
GCP 25	0.21	0.13	0.02	0.47	0.19	0.21
GCP 26	0.22	0.15	0.10	0.26	0.28	0.33
GCP 27	0.26	0.16	0.18	0.42	0.20	0.29
GCP 28	0.22	0.08	0.09	0.32	0.23	0.12
GCP 29	0.12	0.10	0.09	0.32	0.34	0.14
GCP 30	0.13	0.25	0.15	0.32	0.40	0.27
GCP 31	0.06	0.07	0.08	0.29	0.17	0.23
GCP 32	0.23	0.25	0.20	0.49	0.35	0.24
GCP 33	0.18	0.18	0.22	0.35	0.42	0.37
GCP 34	0.26	0.11	0.16	0.27	0.28	0.38
GCP 35	0.16	0.09	0.02	0.32	0.34	0.28
GCP 36	0.03	0.23	0.24	0.22	0.24	0.34
GCP 37	0.03	0.26	0.16	0.29	0.52	0.38
GCP 38	0.19	0.23	0.10	0.30	0.34	0.13
GCP 39	0.09	0.12	0.03	0.27	0.13	0.13
GCP 40	0.06	0.17	0.03	0.12	0.30	0.26
GCP 41	0.08	0.24	0.10	0.15	0.49	0.24
GCP 42	0.10	0.21	0.12	0.30	0.24	0.37
GCP 43	0.07	0.06	0.23	0.11	0.09	0.44
GCP 44	0.26	0.10	0.20	0.39	0.23	0.42
GCP 45	0.12	0.22	0.09	0.21	0.23	0.33
GCP 46	0.24	0.03	0.23	0.32	0.27	0.24
GCP 47	0.09	0.24	0.16	0.25	0.44	0.22
GCP 48	0.18	0.16	0.24	0.35	0.38	0.41
GCP 49	0.04	0.18	0.12	0.12	0.44	0.32
GCP 50	0.03	0.08	0.10	0.23	0.14	0.18
GCP 51	0.25	0.14	0.13	0.34	0.36	0.17
GCP 52	0.01	0.25	0.20	0.15	0.42	0.28
GCP 53	0.12	0.01	0.24	0.34	0.17	0.44
GCP 54	0.18	0.18	0.17	0.23	0.40	0.20
GCP 55	0.05	0.10	0.25	0.08	0.28	0.51
GCP 56	0.03	0.21	0.05	0.06	0.39	0.07
GCP 57	0.15	0.18	0.21	0.21	0.34	0.29
GCP 58	0.17	0.05	0.12	0.21	0.20	0.38
GCP 59	0.22	0.18	0.18	0.40	0.44	0.40
GCP 60	0.14	0.24	0.16	0.22	0.27	0.30

GCP 61	0.19	0.09	0.11	0.28	0.23	0.26
GCP 62	0.20	0.26	0.26	0.24	0.30	0.38
GCP 63	0.11	0.01	0.04	0.22	0.05	0.24
GCP 64	0.18	0.02	0.19	0.29	0.10	0.22
GCP 65	0.23	0.21	0.20	0.32	0.47	0.31
GCP 66	0.16	0.07	0.19	0.18	0.20	0.45
GCP 67	0.23	0.21	0.18	0.25	0.27	0.30
GCP 68	0.10	0.02	0.19	0.26	0.28	0.26
GCP 69	0.18	0.01	0.19	0.20	0.24	0.44
GCP 70	0.18	0.03	0.11	0.27	0.12	0.31
GCP 71	0.17	0.22	0.03	0.31	0.29	0.24
GCP 72	0.11	0.22	0.09	0.12	0.40	0.11
GCP 73	0.04	0.03	0.26	0.18	0.25	0.28
GCP 74	0.03	0.26	0.26	0.15	0.41	0.44
GCP 75	0.15	0.10	0.24	0.19	0.35	0.38
GCP 76	0.19	0.01	0.23	0.32	0.21	0.49
GCP 77	0.15	0.04	0.24	0.24	0.19	0.28
GCP 78	0.19	0.08	0.04	0.26	0.11	0.13
GCP 79	0.05	0.20	0.01	0.24	0.37	0.02
GCP 80	0.21	0.13	0.24	0.22	0.35	0.25
GCP 81	0.17	0.07	0.21	0.24	0.09	0.32
GCP 82	0.17	0.13	0.05	0.28	0.34	0.19
GCP 83	0.05	0.20	0.10	0.22	0.23	0.26
GCP 84	0.06	0.08	0.12	0.10	0.30	0.19
GCP 85	0.07	0.08	0.25	0.28	0.32	0.38
RMSE	0,152144031	0,161419	0,167997	0,266149	0,298766	0,293201

Series from Lund University

Department of Physical Geography and Ecosystem Science

Master Thesis in Geographical Information Science

1. Anthony Lawther: The application of GIS-based binary logistic regression for slope failure susceptibility mapping in the Western Grampian Mountains, Scotland (2008).

2. Rickard Hansen: Daily mobility in Grenoble Metropolitan Region, France. Applied GIS methods in time geographical research (2008).

3. Emil Bayramov: Environmental monitoring of bio-restoration activities using GIS and Remote Sensing (2009).

4. Rafael Villarreal Pacheco: Applications of Geographic Information Systems as an analytical and visualization tool for mass real estate valuation: a case study of Fontibon District, Bogota, Columbia (2009).

5. Siri Oestreich Waage: a case study of route solving for oversized transport: The use of GIS functionalities in transport of transformers, as part of maintaining a reliable power infrastructure (2010).

6. Edgar Pimiento: Shallow landslide susceptibility – Modelling and validation (2010).

7. Martina Schäfer: Near real-time mapping of floodwater mosquito breeding sites using aerial photographs (2010).

8. August Pieter van Waarden-Nagel: Land use evaluation to assess the outcome of the programme of rehabilitation measures for the river Rhine in the Netherlands (2010).

9. Samira Muhammad: Development and implementation of air quality data mart for Ontario, Canada: A case study of air quality in Ontario using OLAP tool. (2010).

10. Fredros Oketch Okumu: Using remotely sensed data to explore spatial and temporal relationships between photosynthetic productivity of vegetation and malaria transmission intensities in selected parts of Africa (2011).

11. Svajunas Plunge: Advanced decision support methods for solving diffuse water pollution problems (2011).

12. Jonathan Higgins: Monitoring urban growth in greater Lagos: A case study using GIS to monitor the urban growth of Lagos 1990 - 2008 and produce future growth prospects for the city (2011).

13. Mårten Karlberg: Mobile Map Client API: Design and Implementation for Android (2011).

14. Jeanette McBride: Mapping Chicago area urban tree canopy using color infrared imagery (2011).

15. Andrew Farina: Exploring the relationship between land surface temperature and vegetation abundance for urban heat island mitigation in Seville, Spain (2011).

16. David Kanyari: Nairobi City Journey Planner: An online and a Mobile Application (2011).

17. Laura V. Drews: Multi-criteria GIS analysis for siting of small wind power plants - A case study from Berlin (2012).

18. Qaisar Nadeem: Best living neighborhood in the city - A GIS based multi criteria evaluation of ArRiyadh City (2012).

19. Ahmed Mohamed El Saeid Mustafa: Development of a photo voltaic building rooftop integration analysis tool for GIS for Dokki District, Cairo, Egypt (2012).

20. Daniel Patrick Taylor: Eastern Oyster Aquaculture: Estuarine Remediation via Site Suitability and Spatially Explicit Carrying Capacity Modeling in Virginia's Chesapeake Bay (2013).

21. Angeleta Oveta Wilson: A Participatory GIS approach to unearthing Manchester's Cultural Heritage 'gold mine' (2013).

22. Ola Svensson: Visibility and Tholos Tombs in the Messenian Landscape: A Comparative Case Study of the Pylian Hinterlands and the Soulima Valley (2013).

23. Monika Ogden: Land use impact on water quality in two river systems in South Africa (2013).

24. Stefan Rova: A GIS based approach assessing phosphorus load impact on Lake Flaten in Salem, Sweden (2013).

25. Yann Buhot: Analysis of the history of landscape changes over a period of 200 years. How can we predict past landscape pattern scenario and the impact on habitat diversity? (2013).

26. Christina Fotiou: Evaluating habitat suitability and spectral heterogeneity models to predict weed species presence (2014).

27. Inese Linuza: Accuracy Assessment in Glacier Change Analysis (2014).

28. Agnieszka Griffin: Domestic energy consumption and social living standards: a GIS analysis within the Greater London Authority area (2014).

29. Brynja Guðmundsdóttir: Detection of potential arable land with remote sensing and GIS - A Case Study for Kjósarhreppur (2014).

30. Oleksandr Nekrasov: Processing of MODIS Vegetation Indices for analysis of agricultural droughts in the southern Ukraine between the years 2000-2012 (2014).

31. Sarah Tressel: Recommendations for a polar Earth science portal in the context of Arctic Spatial Data Infrastructure (2014).

32. Caroline Gevaert: Combining Hyperspectral UAV and Multispectral Formosat-2 Imagery for Precision Agriculture Applications (2014).

33. Salem Jamal-Uddeen: Using GeoTools to implement the multi-criteria evaluation analysis - weighted linear combination model (2014).

34. Samanah Seyedi-Shandiz: Schematic representation of geographical railway network at the Swedish Transport Administration (2014).

35. Kazi Masel Ullah: Urban Land-use planning using Geographical Information System and analytical hierarchy process: case study Dhaka City (2014).

36. Alexia Chang-Wailing Spitteler: Development of a web application based on MCDA and GIS for the decision support of river and floodplain rehabilitation projects (2014).

37. Alessandro De Martino: Geographic accessibility analysis and evaluation of potential changes to the public transportation system in the City of Milan (2014).

38. Alireza Mollasalehi: GIS Based Modelling for Fuel Reduction Using Controlled Burn in Australia. Case Study: Logan City, QLD (2015).

39. Negin A. Sanati: Chronic Kidney Disease Mortality in Costa Rica; Geographical Distribution, Spatial Analysis and Non-traditional Risk Factors (2015).

40. Karen McIntyre: Benthic mapping of the Bluefields Bay fish sanctuary, Jamaica (2015).

41. Kees van Duijvendijk: Feasibility of a low-cost weather sensor network for agricultural purposes: A preliminary assessment (2015).

42. Sebastian Andersson Hylander: Evaluation of cultural ecosystem services using GIS (2015).

43. Deborah Bowyer: Measuring Urban Growth, Urban Form and Accessibility as Indicators of Urban Sprawl in Hamilton, New Zealand (2015).

44. Stefan Arvidsson: Relationship between tree species composition and phenology extracted from satellite data in Swedish forests (2015).

45. Damián Giménez Cruz: GIS-based optimal localisation of beekeeping in rural Kenya (2016).

46. Alejandra Narváez Vallejo: Can the introduction of the topographic indices in LPJ-GUESS improve the spatial representation of environmental variables? (2016).

47. Anna Lundgren: Development of a method for mapping the highest coastline in Sweden using breaklines extracted from high resolution digital elevation models (2016).

48. Oluwatomi Esther Adejoro: Does location also matter? A spatial analysis of social achievements of young South Australians (2016).

49. Hristo Dobrev Tomov: Automated temporal NDVI analysis over the Middle East for the period 1982 - 2010 (2016).

50. Vincent Muller: Impact of Security Context on Mobile Clinic Activities A GIS Multi Criteria Evaluation based on an MSF Humanitarian Mission in Cameroon (2016).

51. Gezahagn Negash Seboka: Spatial Assessment of NDVI as an Indicator of Desertification in Ethiopia using Remote Sensing and GIS (2016).

52. Holly Buhler: Evaluation of Interfacility Medical Transport Journey Times in Southeastern British Columbia. (2016).

53. Lars Ole Grottenberg: Assessing the ability to share spatial data between emergency management organisations in the High North (2016).

54. Sean Grant: The Right Tree in the Right Place: Using GIS to Maximize the Net Benefits from Urban Forests (2016).

55. Irshad Jamal: Multi-Criteria GIS Analysis for School Site Selection in Gorno-Badakhshan Autonomous Oblast, Tajikistan (2016).

56. Fulgencio Sanmartín: Wisdom-volkano: A novel tool based on open GIS and time-series visualization to analyse and share volcanic data (2016).

57.

Nezha Acil: Remote sensing-based monitoring of snow cover dynamics and its influence on vegetation growth in the Middle Atlas Mountains (2016).

58. Julia Hjalmarsson: A Weighty Issue: Estimation of Fire Size with Geographically Weighted Logistic Regression (2016).

59. Mathewos Tamiru Amato: Using multi-criteria evaluation and GIS for chronic food and nutrition insecurity indicators analysis in Ethiopia (2016).

60. Karim Alaa El Din Mohamed Soliman El Attar: Bicycling Suitability in Downtown, Cairo, Egypt (2016).

61. Gilbert Akol Echelai: Asset Management: Integrating GIS as a Decision Support Tool in Meter Management in National Water and Sewerage Corporation (2016).

62. Terje Slinning: Analytic comparison of multibeam echo soundings (2016).

63. Gréta Hlín Sveinsdóttir: GIS-based MCDA for decision support: A framework for wind farm siting in Iceland (2017).

64. Jonas Sjögren: Consequences of a flood in Kristianstad, Sweden: A GIS-based analysis of impacts on important societal functions (2017).

65. Nadine Raska: 3D geologic subsurface modelling within the Mackenzie Plain, Northwest Territories, Canada (2017).

66. Panagiotis Symeonidis: Study of spatial and temporal variation of atmospheric optical parameters and their relation with PM 2.5 concentration over Europe using GIS technologies (2017).

67. Michaela Bobeck: A GIS-based Multi-Criteria Decision Analysis of Wind Farm Site Suitability in New South Wales, Australia, from a Sustainable Development Perspective (2017).

68. Raghdaa Eissa: Developing a GIS Model for the Assessment of Outdoor Recreational Facilities in New Cities Case Study: Tenth of Ramadan City, Egypt (2017).

69. Zahra Khais Shahid: Biofuel plantations and isoprene emissions in Svea and Götaland (2017).

70. Mirza Amir Liaquat Baig: Using geographical information systems in epidemiology: Mapping and analyzing occurrence of diarrhea in urban - residential area of Islamabad, Pakistan (2017).

71. Joakim Jörwall: Quantitative model of Present and Future well-being in the EU-28: A spatial Multi-Criteria Evaluation of socioeconomic and climatic comfort factors (2017).

72. Elin Haettner: Energy Poverty in the Dublin Region: Modelling Geographies of Risk (2017).

73. Harry Eriksson: Geochemistry of stream plants and its statistical relations to soil- and bedrock geology, slope directions and till geochemistry. A GIS-analysis of small catchments in northern Sweden (2017).

74. Daniel Gardevärn: PPGIS and Public meetings – An evaluation of public participation methods for urban planning (2017).

75. Kim Friberg: Sensitivity Analysis and Calibration of Multi Energy Balance Land Surface Model Parameters (2017).

76. Viktor Svanerud: Taking the bus to the park? A study of accessibility to green areas in Gothenburg through different modes of transport (2017).

77. Lisa-Gaye Greene: Deadly Designs: The Impact of Road Design on Road Crash Patterns along Jamaica’s North Coast Highway (2017).

78. Katarina Jemec Parker: Spatial and temporal analysis of fecal indicator bacteria concentrations in beach water in San Diego, California (2017).

79. Angela Kabiru: An Exploratory Study of Middle Stone Age and Later Stone Age Site Locations in Kenya's Central Rift Valley Using Landscape Analysis: A GIS Approach (2017).

80. Kristean Björkmann: Subjective Well-Being and Environment: A GIS-Based Analysis (2018).

81. Williams Erhunmonmen Ojo: Measuring spatial accessibility to healthcare for people living with HIV-AIDS in southern Nigeria (2018).

82. Daniel Assefa: Developing Data Extraction and Dynamic Data Visualization (Styling) Modules for Web GIS Risk Assessment System (WGRAS). (2018).

83. Adela Nistora: Inundation scenarios in a changing climate: assessing potential impacts of sea-level rise on the coast of South-East England (2018).

84. Marc Seliger: Thirsty landscapes - Investigating growing irrigation water consumption and potential conservation measures within Utah's largest master-planned community: Daybreak (2018).

85. Luka Jovičić: Spatial Data Harmonisation in Regional Context in Accordance with INSPIRE Implementing Rules (2018).

86. Christina Kourdounouli: Analysis of Urban Ecosystem Condition Indicators for the Large Urban Zones and City Cores in EU (2018).

87. Jeremy Azzopardi: Effect of distance measures and feature representations on distance-based accessibility measures (2018).

88. Patrick Kabatha: An open source web GIS tool for analysis and visualization of elephant GPS telemetry data, alongside environmental and anthropogenic variables (2018).

89. Richard Alphonce Giliba: Effects of Climate Change on Potential Geographical Distribution of Prunus africana (African cherry) in the Eastern Arc Mountain Forests of Tanzania (2018).

90. Eiður Kristinn Eiðsson: Transformation and linking of authoritative multi-scale geodata for the Semantic Web: A case study of Swedish national building data sets (2018).

91. Niamh Harty: HOP!: a PGIS and citizen science approach to monitoring the condition of upland paths (2018).

92. José Estuardo Jara Alvear: Solar photovoltaic potential to complement hydropower in Ecuador: A GIS-based framework of analysis (2018).

93. Brendan O'Neill: Multicriteria Site Suitability for Algal Biofuel Production Facilities (2018).

94. Roman Spataru: Spatial-temporal GIS analysis in public health – a case study of polio disease (2018).

95. Alicja Miodońska: Assessing evolution of ice caps in Suðurland, Iceland, in years 1986 - 2014, using multispectral satellite imagery (2019).

96. Dennis Lindell Schettini: A Spatial Analysis of Homicide Crime's Distribution and Association with Deprivation in Stockholm Between 2010-2017 (2019).

97. Damiano Vesentini: The Po Delta Biosphere Reserve: Management challenges and priorities deriving from anthropogenic pressure and sea level rise (2019).

98. Emilie Arnesten: Impacts of future sea level rise and high water on roads, railways and environmental objects: a GIS analysis of the potential effects of increasing sea levels and highest projected high water in Scania, Sweden (2019).

99. Syed Muhammad Amir Raza: Comparison of geospatial support in RDF stores: Evaluation for ICOS Carbon Portal metadata (2019).

100. Hemin Tofiq: Investigating the accuracy of Digital Elevation Models from UAV images in areas with low contrast: A sandy beach as a case study (2019).

101. Evangelos Vafeiadis: Exploring the distribution of accessibility by public transport using spatial analysis. A case study for retail concentrations and public hospitals in Athens (2019).

102. Milan Sekulic: Multi-Criteria GIS modelling for optimal alignment of roadway by-passes in the Tlokweng Planning Area, Botswana (2019).

103. Ingrid Piirisaar: A multi-criteria GIS analysis for siting of utility-scale photovoltaic solar plants in county Kilkenny, Ireland (2019).

104. Nigel Fox: Plant phenology and climate change: possible effect on the onset of various wild plant species' first flowering day in the UK (2019).

105. Gunnar Hesch: Linking conflict events and cropland development in Afghanistan, 2001 to 2011, using MODIS land cover data and Uppsala Conflict Data Programme (2019).

106. Elijah Njoku: Analysis of spatial-temporal pattern of Land Surface Temperature (LST) due to NDVI and elevation in Ilorin, Nigeria (2019).

107. Katalin Bunyevácz: Development of a GIS methodology to evaluate informal urban green areas for inclusion in a community governance program (2019).

108. Paul dos Santos: Automating synthetic trip data generation for an agent-based simulation of urban mobility (2019).

109. Robert O' Dwyer: Land cover changes in Southern Sweden from the mid-Holocene to present day: Insights for ecosystem service assessments (2019).

110. Daniel Klingmyr: Global scale patterns and trends in tropospheric NO2 concentrations (2019).

111. Marwa Farouk Elkabbany: Sea Level Rise Vulnerability Assessment for Abu Dhabi, United Arab Emirates (2019).

112. Jip Jan van Zoonen: Aspects of Error Quantification and Evaluation in Digital Elevation Models for Glacier Surfaces (2020).

113. Georgios Efthymiou: The use of bicycles in a mid-sized city – benefits and obstacles identified using a questionnaire and GIS (2020).

114. Haruna Olayiwola Jimoh: Assessment of Urban Sprawl in MOWE/IBAFO Axis of Ogun State using GIS Capabilities (2020).

115. Nikolaos Barmpas Zachariadis: Development of an iOS, Augmented Reality for disaster management (2020).

116. Ida Storm: ICOS Atmospheric Stations: Spatial Characterization of CO2 Footprint Areas and Evaluating the Uncertainties of Modelled CO2 Concentrations (2020).

117. Alon Zuta: Evaluation of water stress mapping methods in vineyards using airborne thermal imaging (2020).

118. Marcus Eriksson: Evaluating structural landscape development in the municipality Upplands-Bro, using landscape metrics indices (2020).

119. Ane Rahbek Vierø: Connectivity for Cyclists? A Network Analysis of Copenhagen's Bike Lanes (2020).

120. Cecilia Baggini: Changes in habitat suitability for three declining Anatidae species in saltmarshes on the Mersey estuary, North-West England (2020).

121. Bakrad Balabanian: Transportation and Its Effect on Student Performance (2020).

122. Ali Al Farid: Knowledge and Data Driven Approaches for Hydrocarbon Microseepage Characterizations: An Application of Satellite Remote Sensing (2020).

123. Bartlomiej Kolodziejczyk: Distribution Modelling of Gene Drive-Modified Mosquitoes and Their Effects on Wild Populations (2020).

124. Alexis Cazorla: Decreasing organic nitrogen concentrations in European water bodies - links to organic carbon trends and land cover (2020).

125. Kharid Mwakoba: Remote sensing analysis of land cover/use conditions of community-based wildlife conservation areas in Tanzania (2021).

126. Chinatsu Endo: Remote Sensing Based Pre-Season Yellow Rust Early Warning in Oromia, Ethiopia (2021).

127. Berit Mohr: Using remote sensing and land abandonment as a proxy for long-term human out-migration. A Case Study: Al-Hassakeh Governorate, Syria (2021).

128. Kanchana Nirmali Bandaranayake: Considering future precipitation in delineation locations for water storage systems - Case study Sri Lanka (2021).

129. Emma Bylund: Dynamics of net primary production and food availability in the aftermath of the 2004 and 2007 desert locust outbreaks in Niger and Yemen (2021).

130. Shawn Pace: Urban infrastructure inundation risk from permanent sea-level rise scenarios in London (UK), Bangkok (Thailand) and Mumbai (India): A comparative analysis (2021).

131. Oskar Evert Johansson: The hydrodynamic impacts of Estuarine Oyster reefs, and the application of drone technology to this study (2021).

132. Pritam Kumarsingh: A Case Study to develop and test GIS/SDSS methods to assess the production capacity of a Cocoa Site in Trinidad and Tobago (2021).

133. Muhammad Imran Khan: Property Tax Mapping and Assessment using GIS (2021).

134. Domna Kanari: Mining geosocial data from Flickr to explore tourism patterns: The case study of Athens (2021).

135. Mona Tykesson Klubien: Livestock-MRSA in Danish pig farms (2021).

136. Ove Njøten: Comparing radar satellites. Use of Sentinel-1 leads to an increase in oil spill alerts in Norwegian waters (2021).

137. Panagiotis Patrinos: Change of heating fuel consumption patterns produced by the economic crisis in Greece (2021).

138. Lukasz Langowski: Assessing the suitability of using Sentinel-1A SAR multi-temporal imagery to detect fallow periods between rice crops (2021).

139. Jonas Tillman: Perception accuracy and user acceptance of legend designs for opacity data mapping in GIS (2022).

140. Gabriela Olekszyk: ALS (Airborne LIDAR) accuracy: Can potential low data quality of ground points be modelled/detected? Case study of 2016 LIDAR capture over Auckland, New Zealand (2022).

141. Luke Aspland: Weights of Evidence Predictive Modelling in Archaeology (2022).

142. Luís Fareleira Gomes: The influence of climate, population density, tree species and land cover on fire pattern in mainland Portugal (2022).

143. Andreas Eriksson: Mapping Fire Salamander (Salamandra salamandra) Habitat Suitability in Baden-Württemberg with Multi-Temporal Sentinel-1 and Sentinel-2 Imagery (2022).

144. Lisbet Hougaard Baklid: Geographical expansion rate of a brown bear population in Fennoscandia and the factors explaining the directional variations (2022).

145. Victoria Persson: Mussels in deep water with climate change: Spatial distribution of mussel (Mytilus galloprovincialis) growth offshore in the French Mediterranean with respect to climate change scenario RCP 8.5 Long Term and Integrated Multi-Trophic Aquaculture (IMTA) using Dynamic Energy Budget (DEB) modelling (2022).

146. Benjamin Bernard Fabien Gérard Borgeais: Implementing a multi-criteria GIS analysis and predictive modelling to locate Upper Palaeolithic decorated caves in the Périgord noir, France (2022).

147. Bernat Dorado-Guerrero: Assessing the impact of post-fire restoration interventions using spectral vegetation indices: A case study in El Bruc, Spain (2022).

148. Ignatius Gabriel Aloysius Maria Perera: The Influence of Natural Radon Occurrence on the Severity of the COVID-19 Pandemic in Germany: A Spatial Analysis (2022).

149. Mark Overton: An Analysis of Spatially-enabled Mobile Decision Support Systems in a Collaborative Decision-Making Environment (2022).

150. Viggo Lunde: Analysing methods for visualizing time-series datasets in open-source web mapping (2022).

151. Johan Viscarra Hansson: Distribution Analysis of Impatiens glandulifera in Kronoberg County and a Pest Risk Map for Alvesta Municipality (2022).

152. Vincenzo Poppiti: GIS and Tourism: Developing strategies for new touristic flows after the Covid-19 pandemic (2022).

153. Henrik Hagelin: Wildfire growth modelling in Sweden - A suitability assessment of available data (2023).

154. Gabriel Romeo Ferriols Pavico: Where there is road, there is fire (influence): An exploratory study on the influence of roads in the spatial patterns of Swedish wildfires of 2018 (2023).

155. Colin Robert Potter: Using a GIS to enable an economic, land use and energy output comparison between small wind powered turbines and large-scale wind farms: the case of Oslo, Norway (2023).

156. Krystyna Muszel: Impact of Sea Surface Temperature and Salinity on Phytoplankton blooms phenology in the North Sea (2023).

157. Tobias Rydlinge: Urban tree canopy mapping - an open source deep learning approach (2023).

158. Albert Wellendorf: Multi-scale Bark Beetle Predictions Using Machine Learning (2023).

159. Manolis Papadakis: Use of Satellite Remote Sensing for Detecting Archaeological Features: An Example from Ancient Corinth, Greece (2023).

160. Konstantinos Sourlamtas: Developing a Geographical Information System for a water and sewer network, for monitoring, identification and leak repair - Case study: Municipal Water Company of Naoussa, Greece (2023).